

Supporting Information

for

A Revised Understanding of the Speciation of Gold(III) Dithiocarbamate Complexes in Solution

Ryan K. Brown,^{a§} Joseph N. Bunyan,^{a§} Ashi Agrawal,^a Guoyu Li,^a Dominykas Dautoras,^a
Jagodish C. Sarker,^{a,b} Terng Tor Keat,^a Thomas Hicks,^a Graeme Hogarth,^a and David Pugh^{*a}

a: Department of Chemistry, King's College London, Britannia House, 7 Trinity Street, London, SE1 1DB, UK.

b: Department of Chemistry, Jagannath University, Dhaka 1100, Bangladesh

E-mail David.Pugh@kcl.ac.uk

§ = these authors contributed equally

Contents

1. General experimental details	S2
2. Crystallographic information	S3
3. NMR spectra	S11
4. Other spectra	S43
5. References	S45

1. General Experimental Details

1.1 Materials

Syntheses were conducted in air using standard grade non-dried solvents (analar-grade acetone). Deionized water was obtained from an Elga Purelab Option-R 7/15.

Na[AuCl₄], K[AuCl₄], anhydrous AuBr₃ (all Fisher), H[AuCl₄], Na(Me₂dtc)·2(H₂O), Na(Et₂dtc)·3(H₂O) and CS₂ (all Sigma/Merck) were purchased from the companies indicated and used as received. Secondary amines were purchased from common suppliers (typically Sigma/Merck, Fisher, or VWR) and distilled from CaH₂ prior to use unless they were already colorless and pure by ¹H NMR spectroscopy. Silica gel (technical grade, 300–400 mesh particle size) for column chromatography and Celite® were both purchased from Fisher.

Na(dtc) and K(dtc) salts were synthesized by a standard literature procedure.^{S1} Identities and purity of products were confirmed through comparison to known literature data: Na(*t*Pr₂dtc),^{S2} K(*t*Bu₂dtc),^{S3} Na(pyrr-dtc),^{S4} Na(pip-dtc).^{S5} Li(p-tolyl₂dtc) was synthesized from a literature procedure.^{S6} [AuCl(tht)] was synthesised from H[AuCl₄] by a literature procedure.^{S7} Au(I) dithiocarbamate complexes were synthesized by reacting M(dtc) with one molar equivalent of [AuCl(tht)] in CH₂Cl₂. A coloured suspension formed which was stirred for 24 hours, then isolated by filtration, washed with CH₂Cl₂ (3 x 5 mL) and dried *in vacuo*. The purity of [Au(Et₂dtc)]_n was confirmed by comparison of ¹H NMR spectroscopic data to literature data.^{S8}

1.2 Instrumentation

¹H NMR and ¹³C{¹H} NMR spectra were recorded at 298 K on a Bruker Ascend 400 spectrometer operating at 400.1 MHz (¹H). Spectra were obtained in CDCl₃, (CD₃)₂CO, CD₃CN, or (CD₃)₂SO (all used as received from Merck) and are referenced to the residual protio-solvent signal. The reported values for ¹H and ¹³C{¹H} NMR data are as follows: chemical shift (δ, ppm), multiplicity (where s = singlet, d = doublet, t = triplet, m = multiplet), integration (not ¹³C), and coupling constant (*J*, Hz). DEPT-135 and 2D correlation experiments (COSY, HSQC) were sometimes used to aid signal assignment but have not been documented below.

UV-vis spectra were obtained on an Agilent Cary 100 spectrometer.

Elemental analysis was obtained at London Metropolitan University.

2. Crystallographic Information

2.1 General Methods and Instrumentation

We thank the EPSRC UK National Crystallography Service at the University of Southampton for collection of some of the crystallographic data.^{S9} Hardware used: a Rigaku FRE⁺ diffractometer (Mo-K_α radiation, 0.71073 Å) equipped with HF Varimax confocal mirrors, an AFC12 goniometer, HG Saturn 724⁺ detector, and an Oxford Cryosystems low-temperature device operating at 100(1) K.

For [AuBr₂(p-tolyl₂dtc)], [Au(p-tolyl₂dtc)][AuBr₂] and [AuBr₂(Et₂dtc)], data was collected on an Oxford Diffraction Xcalibur S single-crystal diffractometer operating at 150(1) K with a Sapphire 3 CCD plate (graphite-monochromated Mo K_α radiation, λ = 0.71073 Å), or graphite-monochromated Cu K_α radiation, λ = 1.54184 Å for [AuCl₂(p-tolyl₂dtc)] and [Au(Me₂dtc)₂][AuBr₂].

Datasets were processed using CrysAlisPro^{S13} and solutions were solved and refined using Olex-2.^{S14} Graphics were generated using Olex-2 and Mercury.^{S15} CCDC reference numbers 2374277 [AuCl₂(*i*-Pr₂dtc)], 2374278 [AuCl₂(*i*-Bu₂dtc)], 2374279 [Au(*i*-Bu₂dtc)₂][AuCl₂], 2374280 [AuCl₂(p-tolyl₂dtc)], 2374281 [Au(p-tolyl₂dtc)][AuCl₂], 2374282 [AuBr₂(p-tolyl₂dtc)], 2374283 [Au(p-tolyl₂dtc)][AuBr₂], 2374284 [AuBr₂(Et₂dtc)], 2374285 [Au(Et₂dtc)₂][AuBr₂], 2374286 [Au(Et₂dtc)₂][BF₄], 2374287 [AuBr₂(Me₂dtc)], 2374288 [Au(Me₂dtc)₂][AuBr₂] contain crystallographic data in CIF format, which is summarized in Table S1.

Table S1: CIF data for the X-ray structures reported in this paper.

	[AuCl ₂ (ⁱ Pr ₂ dtc)]	[AuCl ₂ (ⁱ Bu ₂ dtc)]	[Au(ⁱ Bu ₂ dtc) ₂] [AuCl ₂]	[AuCl ₂ (p-tolyl ₂ dtc)]	[Au(p-tolyl ₂ dtc) ₂] [AuCl ₂]·CH ₂ Cl ₂	[AuBr ₂ (p-tolyl ₂ dtc)]
Empirical formula	C ₇ H ₁₄ AuCl ₂ NS ₂	C ₉ H ₁₈ AuCl ₂ NS ₂	C ₁₈ H ₃₆ Au ₂ Cl ₂ N ₂ S ₄	C ₁₅ H ₁₄ AuCl ₂ NS ₂	C ₃₁ H ₃₀ Au ₂ Cl ₄ N ₂ S ₄	C ₁₅ H ₁₄ AuBr ₂ NS ₂
Formula weight (Å)	444.18	472.23	873.56	540.26	1094.54	629.18
Crystal system	orthorhombic	monoclinic	triclinic	monoclinic	triclinic	monoclinic
Space group	<i>Pnma</i>	<i>P2₁/n</i>	<i>P</i> -1	<i>C2/c</i>	<i>P</i> -1	<i>C2/c</i>
<i>a</i> (Å)	14.2861(4)	16.8266(3)	8.1079(2)	17.7475(4)	9.4231(1)	19.2273(6)
<i>b</i> (Å)	8.4355(3)	11.09752(12)	13.3585(2)	12.8512(3)	13.6971(3)	10.0252(2)
<i>c</i> (Å)	10.3479(3)	16.8429(3)	13.5963(3)	7.69468(18)	14.0103(3)	19.6140(6)
<i>α</i> (°)	90	90	76.596(2)	90	100.096(2)	90
<i>β</i> (°)	90	108.4251(17)	77.724(2)	97.150(2)	92.064(1)	105.615(3)
<i>γ</i> (°)	90	90	84.299(2)	90	96.601(2)	90
Volume (Å ³)	1247.03(7)	2983.91(8)	1397.80(5)	1741.33(7)	1765.58(6)	3641.21(18)
Z	4	8	2	4	2	8
Density (calc.) (g/cm ³)	2.366	2.102	2.076	2.061	2.059	2.295
Absorption coefficient	12.519	10.471	10.982	20.869	8.864	12.691
F(000)	832	1792	828	1024	1040	2336
2θ range (°)	6.23 to 54.97	5.97 to 50.05	3.14 to 63.21	10.05 to 72.17	2.96 to 65.94	5.90 to 59.93
Reflections collected	40643	59414	74105	4062	221617	9055
Independent reflections	1530	5235	8622	1716	12633	4626
Data / restraints / parameters	1530/0/76	5235/0/280	8622/0/265	1716/0/98	12633/0/395	4626/0/192
Goodness-of-fit on <i>F</i> ²	1.124	1.103	1.022	1.045	1.041	1.027
Final <i>R</i> indices [<i>I</i> >2σ(<i>I</i>)]	R ₁ = 0.0161 wR ₂ = 0.0370	R ₁ = 0.0250 wR ₂ = 0.0625	R ₁ = 0.0187 wR ₂ = 0.0395	R ₁ = 0.0323 wR ₂ = 0.0737	R ₁ = 0.0266 wR ₂ = 0.0578	R ₁ = 0.0373 wR ₂ = 0.0599
<i>R</i> indices (all data)	R ₁ = 0.0178 wR ₂ = 0.0375	R ₁ = 0.0254 wR ₂ = 0.0626	R ₁ = 0.0224 wR ₂ = 0.0403	R ₁ = 0.0351 wR ₂ = 0.0752	R ₁ = 0.0341 wR ₂ = 0.0597	R ₁ = 0.0499 wR ₂ = 0.0645
Largest peak/hole (eÅ ⁻³)	1.50/-1.44	4.56/-1.20	1.28/-0.93	1.31/-0.93	4.84/-1.76	1.63/-1.11

Table S1 (cont.)

	[Au(p-tolyl₂dtc)₂] [AuBr₂]·CH₂Cl₂	[AuBr₂(Et₂dtc)]	[Au(Et₂dtc)₂] [AuBr₂]	[Au(Et₂dtc)₂] [BF₄]	[AuBr₂(Me₂dtc)]	[Au(Me₂dtc)₂] [AuBr₂]
Empirical formula	C ₃₁ H ₃₀ Au ₂ Br ₂ Cl ₂ N ₂ S ₄	C ₅ H ₁₀ AuBr ₂ NS ₂	C ₁₀ H ₂₀ Au ₂ Br ₂ N ₂ S ₄	C ₁₀ H ₂₀ AuBF ₄ N ₂ S ₄	C ₃ H ₆ AuBr ₂ NS ₂	C ₆ H ₁₂ Au ₂ Br ₂ N ₂ S ₄
Formula weight (Å)	1183.46	505.05	850.27	580.30	476.99	794.17
Crystal system	triclinic	monoclinic	monoclinic	monoclinic	monoclinic	monoclinic
Space group	<i>P</i> -1	<i>P</i> 2 ₁	<i>C</i> 2/ <i>c</i>	<i>C</i> 2/ <i>c</i>	<i>P</i> 2/ <i>m</i>	<i>C</i> 2/ <i>c</i>
<i>a</i> (Å)	9.6057(3)	7.2901(2)	11.1024(2)	10.9691(1)	6.7854(3)	27.040(3)
<i>b</i> (Å)	13.9353(5)	14.3937(4)	8.9010(1)	7.5079(1)	6.8958(2)	6.0764(2)
<i>c</i> (Å)	14.0539(3)	10.5320(3)	20.2871(3)	21.3469(3)	10.2472(4)	15.3889(19)
α (°)	99.425(2)	90	90	90	90	90
β (°)	92.426(2)	92.846(2)	106.552(2)	90.307(1)	108.353(4)	142.55(3)
γ (°)	97.391(2)	90	90	90	90	90
Volume (Å ³)	1836.55(10)	1103.78(5)	1921.74(5)	1758.00(4)	455.09(3)	1537.4(6)
Z	2	4	4	4	2	4
Density (calc.) (g/cm ³)	2.140	3.039	2.939	2.193	3.481	3.431
Absorption coefficient	10.552	20.891	19.835	8.875	25.324	46.357
F(000)	1112	912	1544	1112	424	1416
2 θ range (°)	5.58 to 60.52	6.27 to 50.05	5.95 to 54.94	3.82 to 72.63	4.19 to 75.87	10.76 to 142.89
Reflections collected	19942	4884	45325	69540	21355	2449
Independent reflections	9419	3165	2204	4259	2551	1453
Data / restraints / parameters	9419/6/395	3165/1/205	2204/0/95	4259/0/105	2551/0/57	1453/0/77
Goodness-of-fit on <i>F</i> ²	1.053	1.071	1.080	1.069	1.020	1.174
Final <i>R</i> indices [<i>I</i> >2 σ (<i>I</i>)]	R ₁ = 0.0316 wR ₂ = 0.0566	R ₁ = 0.0423 wR ₂ = 0.1050	R ₁ = 0.0191 wR ₂ = 0.0523	R ₁ = 0.0143 wR ₂ = 0.0305	R ₁ = 0.0186 wR ₂ = 0.0342	R ₁ = 0.0636 wR ₂ = 0.1580
<i>R</i> indices (all data)	R ₁ = 0.0420 wR ₂ = 0.0598	R ₁ = 0.0440 wR ₂ = 0.1065	R ₁ = 0.0194 wR ₂ = 0.0525	R ₁ = 0.0191 wR ₂ = 0.0317	R ₁ = 0.0236 wR ₂ = 0.0351	R ₁ = 0.0666 wR ₂ = 0.1605
Largest peak/hole (e.Å ⁻³)	1.88/-0.99	2.74/-2.31	2.15/-1.59	0.84/-0.99	1.64/-1.98	2.90/-2.94

2.2 Additional crystallographic experimental details

Many of the structure solutions contained large areas of residual electron density located close to a heavy atom (typically Au, but occasionally Cl, S, Br). This led to Level A and Level B alerts in CheckCIF. Unless stated otherwise below, these areas of electron density are absorption effects and are commonly seen in structures with heavy atoms. In all cases we attempted to refine the absorption correction in post-collection processing but were not able to remove all the absorption peaks.

[AuCl₂(*i*Bu₂dtc)] crystallized with two symmetry-independent molecules in the unit cell. The crystal chosen was also a twin, with twin law [0 0 1 0 -1 0 1 0 0] and a 2:3 ratio of components. No other restraints were required, although large areas of residual electron density were located close to the Au centres which explains the level B alerts in CheckCIF. This is likely due to absorption effects due to the presence of a very heavy atom (Au).

[Au(*i*Bu₂dtc)₂][AuCl₂] also crystallized with two symmetry-independent ion pairs in the unit cell. Both the Au(III) centres were located on inversion points which meant the asymmetric unit consisted of two halves of [Au(*i*Bu₂dtc)₂]⁺ cations and a single linear Au(I) [AuCl₂]⁻ anion.

[Au(p-tolyl₂dtc)₂][AuCl₂] crystallized with a single molecule of CH₂Cl₂ in the asymmetric unit. This was oriented such that it was taking part in hydrogen bonding to the [AuCl₂]⁻ anion with a CH...Cl distance of 2.774 Å and CH...Cl angle of 145.51°. Also, a single area of residual electron density ~3.7 was located very close to Au2 (the Au(I) centre). This suggested disorder of the [AuCl₂]⁻ anion which modelled at around 2% occupancy, but it required strong restraints hence the non-disordered structure is presented. This explains the level B alert in CheckCIF.

[Au(p-tolyl₂dtc)₂][AuBr₂] also crystallized with two symmetry-independent ion pairs in the unit cell. There was also a single molecule of CH₂Cl₂ in the asymmetric unit, but there were no hydrogen bonding interactions of note.

Despite multiple attempts, it was not possible to obtain single crystals of [AuBr₂(Et₂dtc)]. The best dataset was not particularly good quality but did still give a reasonable solution. It was refined as a two-component inversion twin with a 61:39 ratio of components. Several areas of residual electron density remained close to the heavy atoms even after multiple attempts at absorption corrections, which explains the level A and B alerts in CheckCIF.

Several areas of residual electron density remained in [Au(Et₂dtc)₂][AuBr₂] after all the atoms were assigned. Most were close to a heavy atom (Au/Br) but repeated attempts at rerunning the absorption correction failed to remove or reduce the magnitude of these. One area of residual density was not close to a heavy atom and in fact lay on a symmetry operation at (0.75 0.25 0.50). This is too close to C5 to be a solvent such as water, and it is not part of the molecule as determined by other analytical and spectroscopic measurements. No signs of twinning were observed. The most likely explanation for this is a tiny crystallite stuck to the main crystal. It was noted during crystal mounting that the yellow plates were intergrown and had to be cut to

obtain a single crystal. It is most likely that a tiny crystallite was not removed from the main crystal at this point.

[Au(Et₂dtc)₂][BF₄] was refined as a 2-component twin, with twin law [-1 0 0 0 -1 0 0 0 1] and BASF 0.0699(7).

[Au(Me₂dtc)₂][AuBr₂] contained some large residuals close to a heavy atom. The most likely explanation for these is a minor twin component, although we were unable to detect any feasible twin law during refinement.

There were no special details of note for [AuCl₂(p-tolyl₂dtc)], [AuBr₂(Me₂dtc)] or [AuBr₂(p-tolyl₂dtc)].

2.3 Further discussion of intermolecular interactions

The dataset for [AuCl₂(*i*Pr₂dtc)] was collected at a lower temperature than the existing literature dataset.^{S16} Although a slight contraction in the unit cell parameters of our structure was present, there was little difference in the other metrics between the two datasets. The structure itself is mostly unremarkable, with Au–Cl and Au–S distances consistent with other examples of [AuCl₂(dtc)] structures (see main manuscript for references), although the *i*Pr₂dtc ligand adopted an unusual conformation in the solid state (Figure S1). One of the *i*Pr groups rotated such that the methine CH (H2) pointed towards the nearest sulfur atom (CH···S distance = 2.469 Å; CH···S angle = 117.31°). The origin of this effect is not known, but it was similarly observed in the X-ray structure of Na(*i*Pr₂dtc).^{S17} No aurophilic interactions were observed (closest Au···Au distance = 8.435 Å) and no CH···Au interactions were observed in the extended structure.

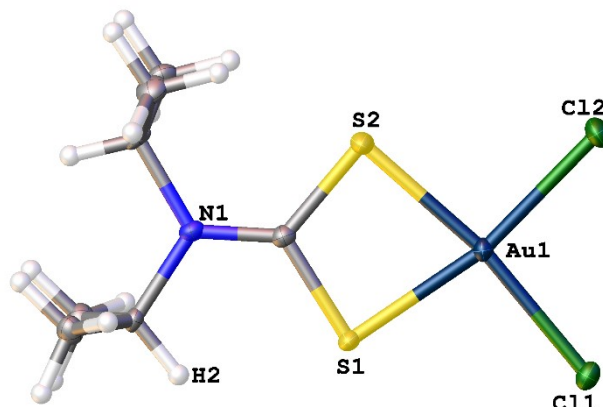


Figure S1: X-ray structure of [AuCl₂(*i*Pr₂dtc)]. Selected bond lengths (Å): Au–Cl1 2.3161(9); Au–Cl2 2.3285(9); Au–S1 2.3002(9); Au–S2 2.2801(9).

The crystal structure of $[\text{AuBr}_2(\text{Me}_2\text{dte})]$ is unremarkable. Long-range $\text{Au}\cdots\text{S}$ interactions of 3.473 Å result from the extended packing of the molecule forming stacked columns. No aurophilic interactions are present; the closest $\text{Au}\cdots\text{Au}$ distance is 4.396 Å. Similarly, the structure of $[\text{Au}(\text{Me}_2\text{dte})_2][\text{AuBr}_2]$ does not contain many interactions of note. There are short contacts between the sulfur atoms on the cation and the Au(I) centre of the anion (3.364 Å) as well as long-range chalcogen bonding between the bromide of the anion and a sulfur on the cation ($\text{Br}\cdots\text{S} = 3.512$ Å; $\angle\text{Br}\cdots\text{S}-\text{C} = 175.5^\circ$).

The structure of $[\text{AuBr}_2(\text{Et}_2\text{dte})]$ contains two symmetry-independent square planar molecules in the asymmetric unit which are stacked in an antiparallel fashion. The Au–S and Au–Br bond lengths are consistent with other Au(III) dithiocarbamate complexes. The packing in this structure is dominated by columns of stacked antiparallel molecules with interactions between Au and S on neighbouring molecules, with $\text{Au}\cdots\text{S}$ distances of 3.443(4), 3.446(4), 3.885(4), 3.903(4) Å (Figure S2).

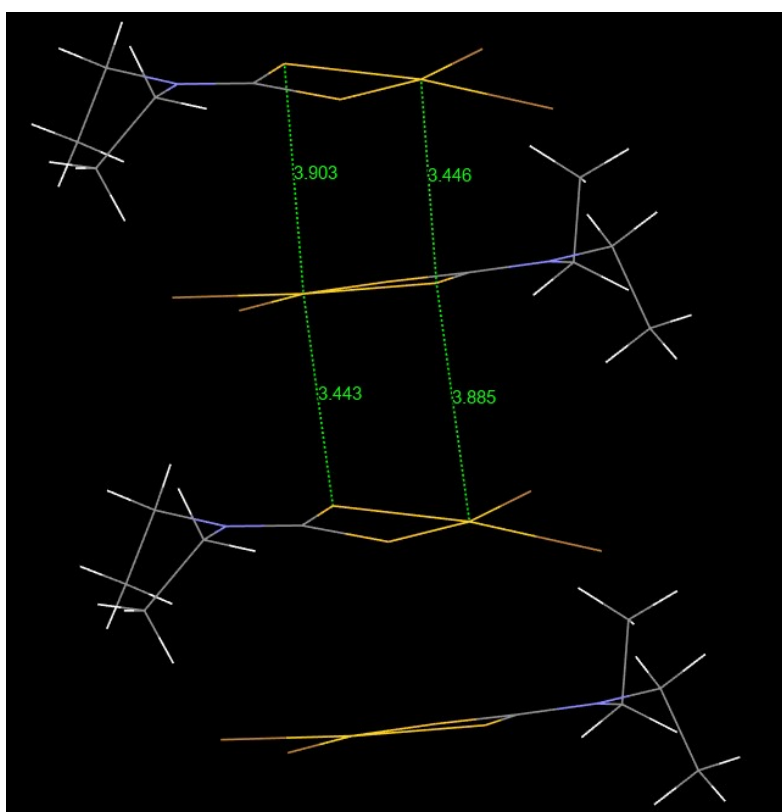


Figure S2: the major intermolecular interactions in $[\text{AuBr}_2(\text{Et}_2\text{dte})]$.

The structure of $[\text{AuBr}_2(\text{Et}_2\text{dte})]$ contains a charge-separated ion pair with square planar Au(III) cation and linear Au(I) anion in the asymmetric unit. The Au–Br and Au–S bond lengths are consistent with other examples of Au(III) dithiocarbamate complexes, and the intermolecular interactions are not especially noteworthy.

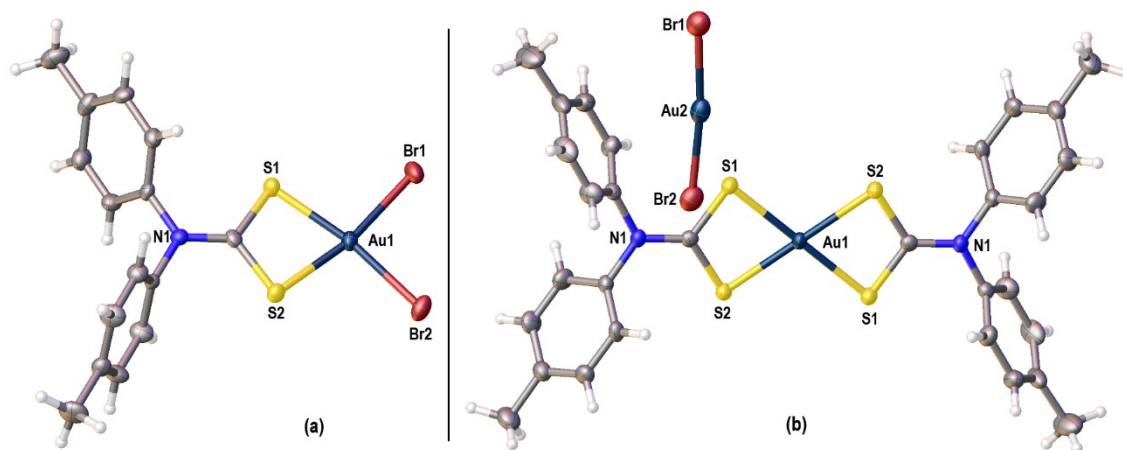


Figure S3 – (a) Solid-state molecular structure of $[\text{AuBr}_2(\text{p-tolyl}_2\text{dtc})]$. Selected bond lengths (\AA): Au1–S1 2.3097(13); Au1–S2 2.3155(13); Au1–Br1 2.4438(6); Au1–Br2 2.4404(6); (b) Solid-state molecular structure of $[\text{Au}(\text{p-tolyl}_2\text{dtc})_2][\text{AuBr}_2]$ showing the Au1-centred ion pair. Range of Au–S bond lengths (\AA): 2.3299(9)–2.3372(9).

The structure of $[\text{AuBr}_2(\text{p-tolyl}_2\text{dtc})]$ (Figure S3a) contains a single square planar Au(III) molecule in the asymmetric unit. The Au–Br and Au–S bond lengths are consistent with other examples of Au(III) dithiocarbamate complexes, and the intermolecular interactions are not especially noteworthy either. There is one short intermolecular Au \cdots S contact of 3.662 \AA but no aurophilic interactions; the shortest Au \cdots Au contact is 4.3207 \AA (Figure S4).

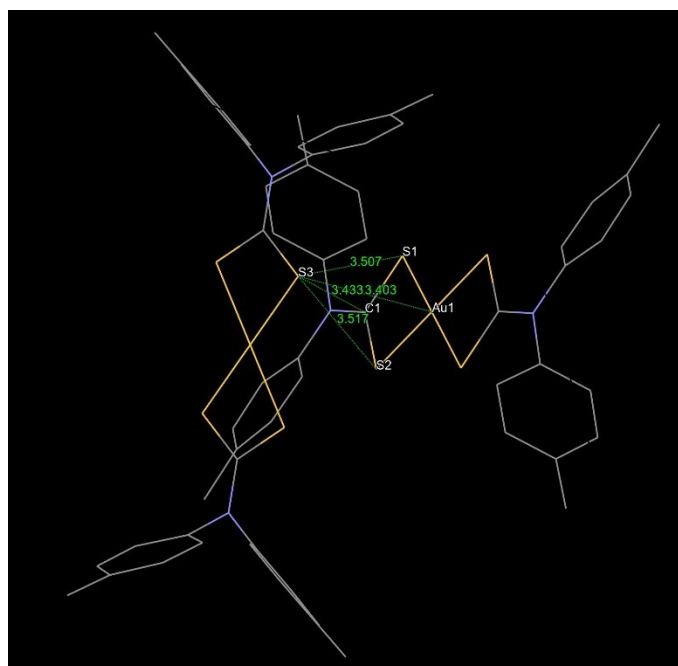


Figure S4: the major intermolecular interactions in $[\text{Au}(\text{p-tolyl}_2\text{dtc})_2][\text{AuBr}_2]$.

The packing in $[\text{Au}(\text{p-tolyl}_2\text{dtc})_2][\text{AuBr}_2]$ is dominated by the lone pair on one sulfur atom (S3) pointing towards the AuS₂C 4-membered ring on a neighbouring cation (based on Au1). There is one short Au \cdots S contact of 3.403 \AA between neighbouring molecules but no aurophilic interactions are present; the shortest Au \cdots Au contact is 4.8029 \AA .

The structure of $[\text{Au}(\text{Et}_2\text{dtc})_2][\text{BF}_4]$ (Figure S5) is unremarkable. The Au–S distances are consistent with other examples of Au–S distances in this study, and there are no interactions between cation and anion. The only long-range interactions present are between the CH_2 hydrogens on one cation and a gold centre on a neighbouring cation, but the $\text{CH}\cdots\text{Au}$ distances of 3.395 and 3.405 Å are long, and there is little directionality to this interaction.

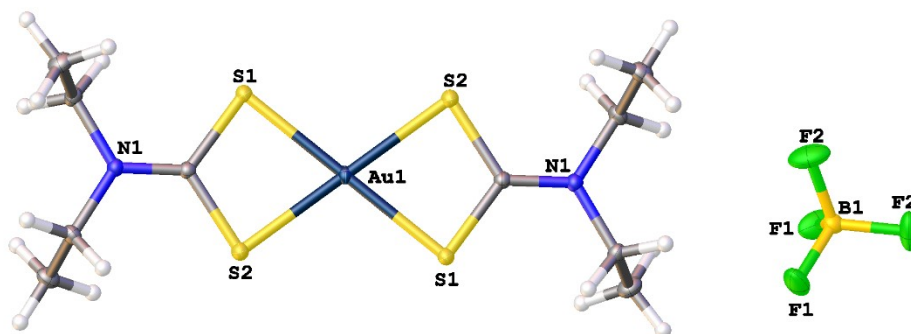


Figure S5: X-ray structure of $[\text{Au}(\text{Et}_2\text{dtc})_2][\text{BF}_4]$. Selected bond lengths (Å): Au–S1 2.3354(3); Au–S2 2.3317(3).

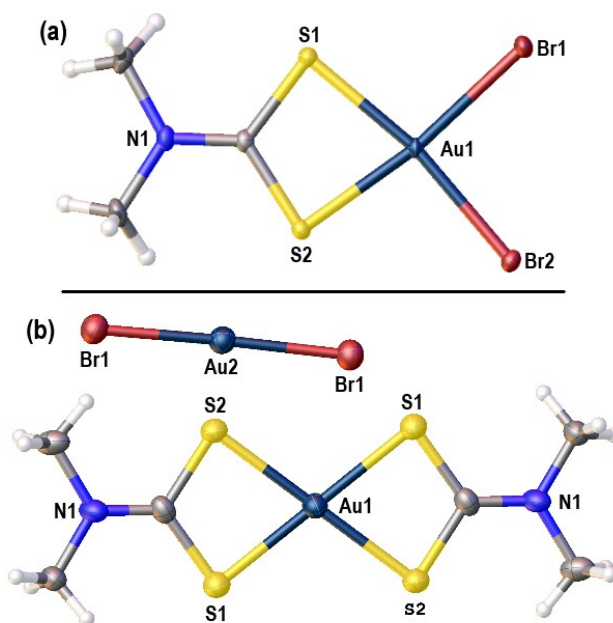


Figure S6 – (a) Solid-state molecular structure of $[\text{AuBr}_2(\text{Me}_2\text{dtc})]$. Selected bond lengths (Å): Au1–S1 2.3240(7); Au1–S2 2.3155(7); Au1–Br1 2.4442(3); Au1–Br2 2.4459(3); (b) Solid-state molecular structure of $[\text{Au}(\text{Me}_2\text{dtc})_2][\text{AuBr}_2]$ showing the Au1-centred ion pair. Selected bond lengths (Å): Au1–S1 2.342(3); Au1–S2 2.343(3); Au1–Br1 2.3949(15).

3. NMR Spectra

3.1 NMR spectra of $[\text{AuX}_2(\text{dte})]/[\text{Au}(\text{dte})_2]^+$ mixtures from aqueous synthesis

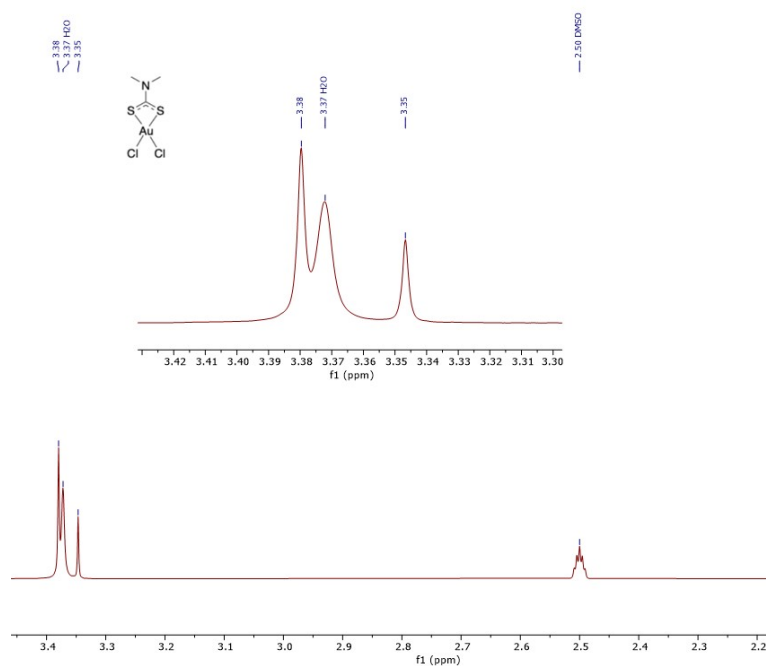


Figure S7: ^1H NMR spectrum of “[$\text{AuCl}_2(\text{Me}_2\text{dte})$]” in DMSO-d_6 . The peak at 3.38 ppm overlaps with the HDO contaminant from the deuterated solvent.

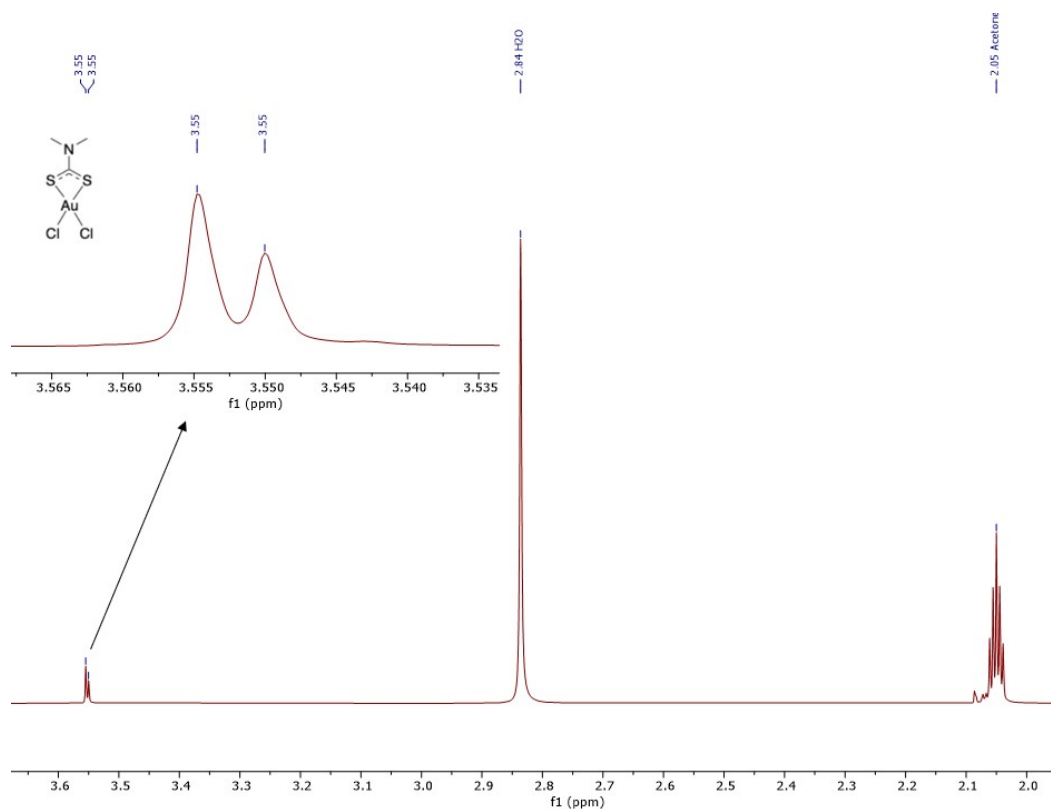


Figure S8: ^1H NMR spectrum of “[$\text{AuCl}_2(\text{Me}_2\text{dte})$]” in $(\text{CD}_3)_2\text{CO}$.

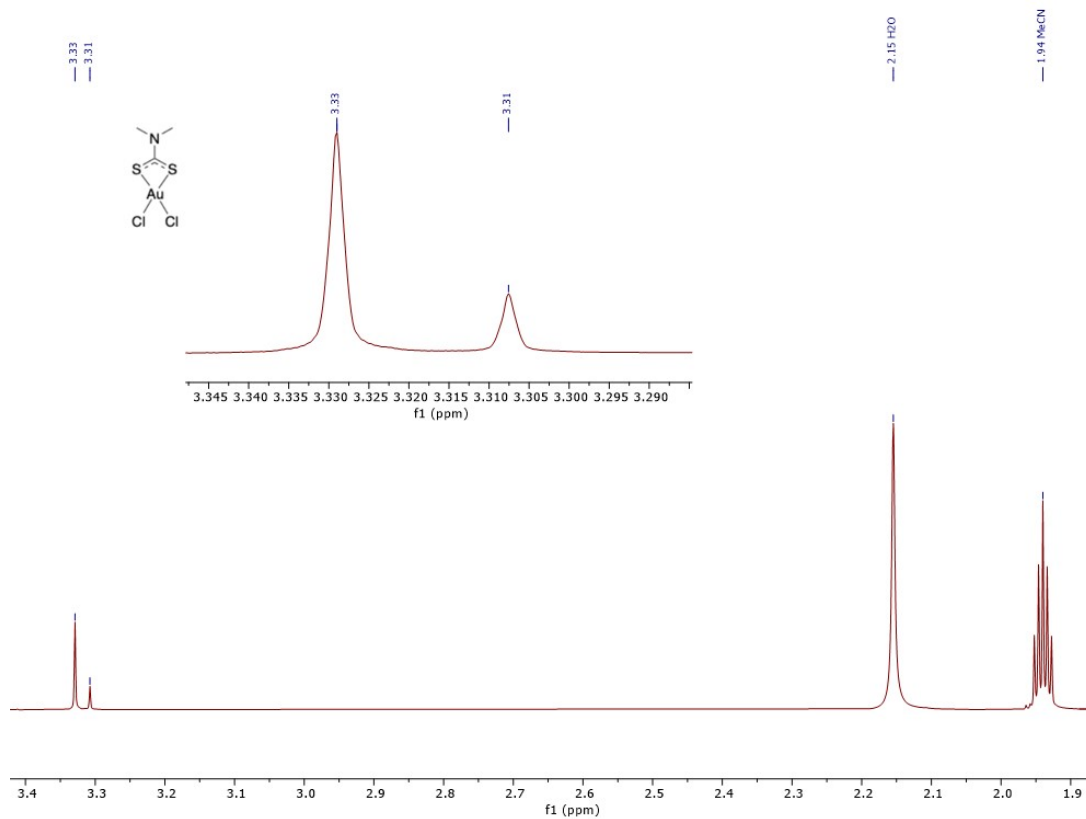


Figure S9: ^1H NMR spectrum of “ $[\text{AuCl}_2(\text{Me}_2\text{dtc})]$ ” in CD_3CN .

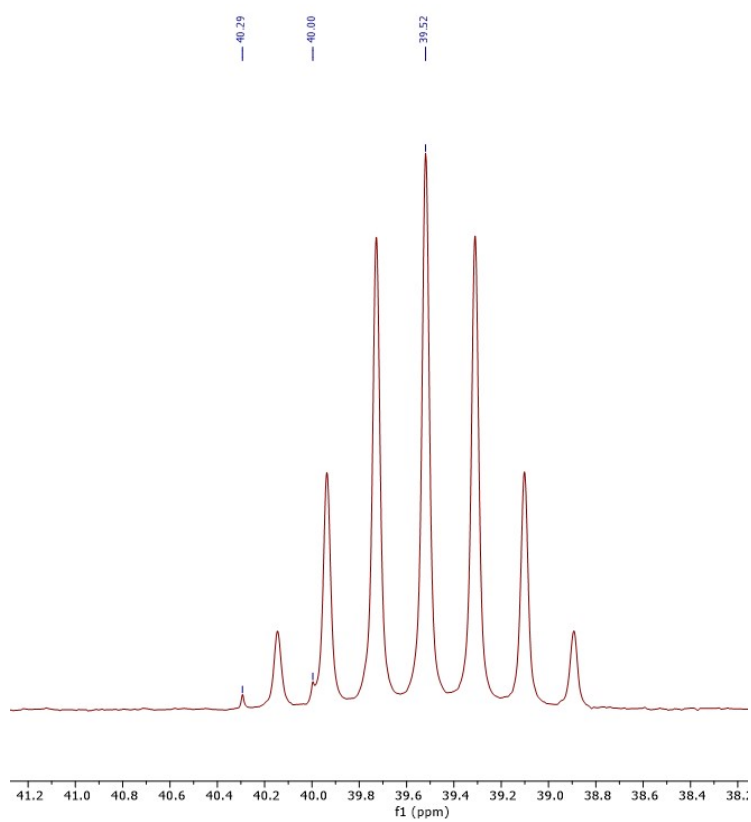


Figure S10: $^{13}\text{C}\{^1\text{H}\}$ NMR spectrum of “ $[\text{AuCl}_2(\text{Me}_2\text{dtc})]$ ” in DMSO-d_6 .

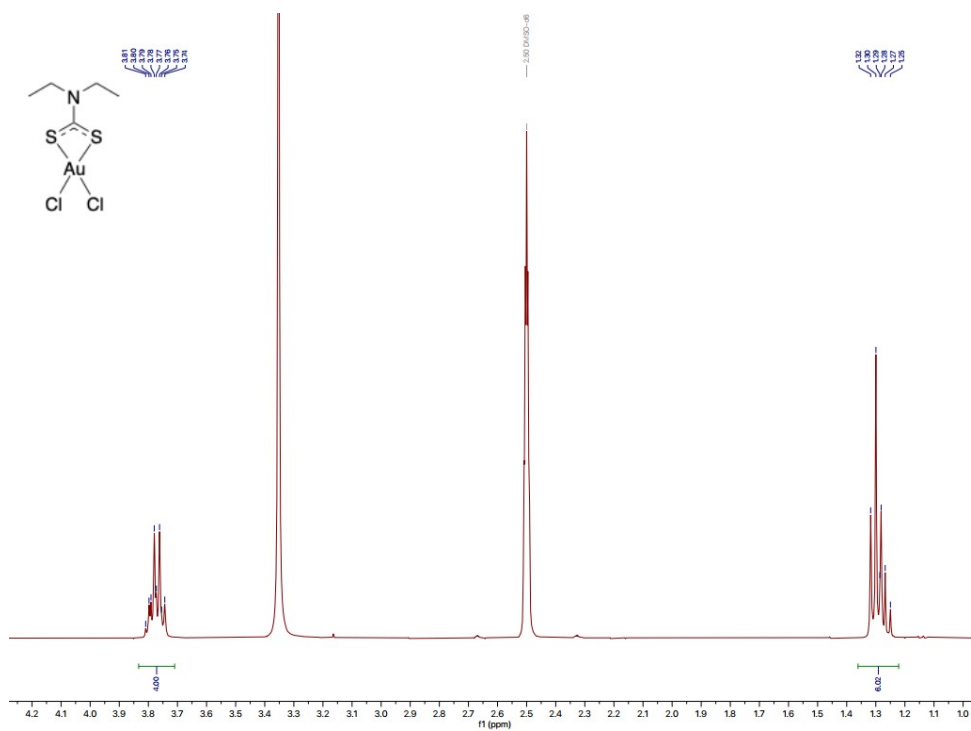


Figure S11: ^1H NMR spectrum of “[AuCl₂(Et₂dtc)]” in DMSO-d₆.

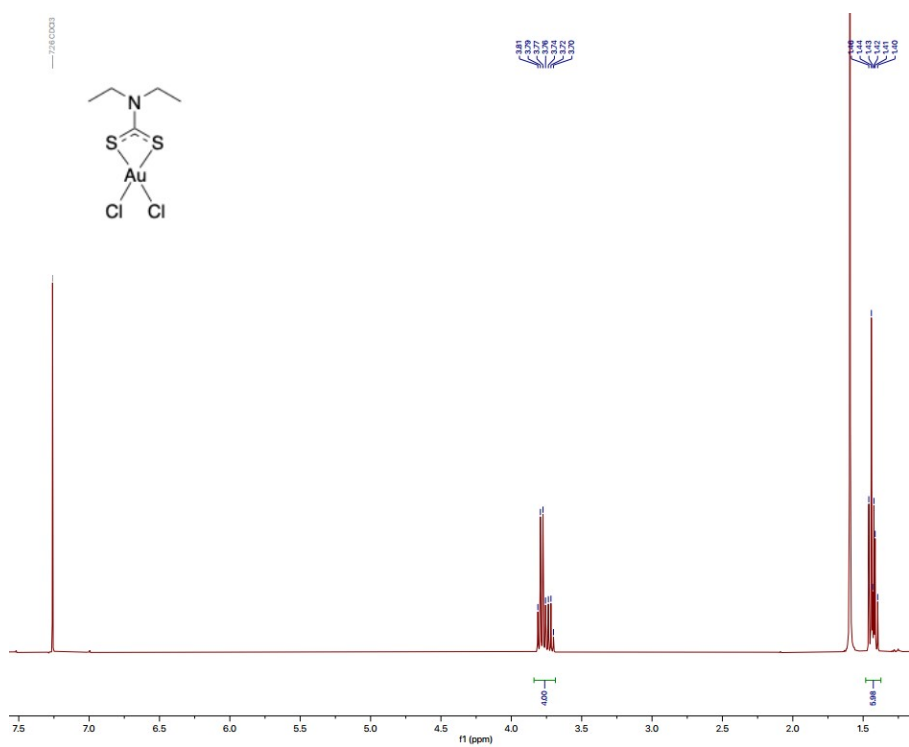


Figure S12: ^1H NMR spectrum of “[AuCl₂(Et₂dtc)]” in CDCl₃.

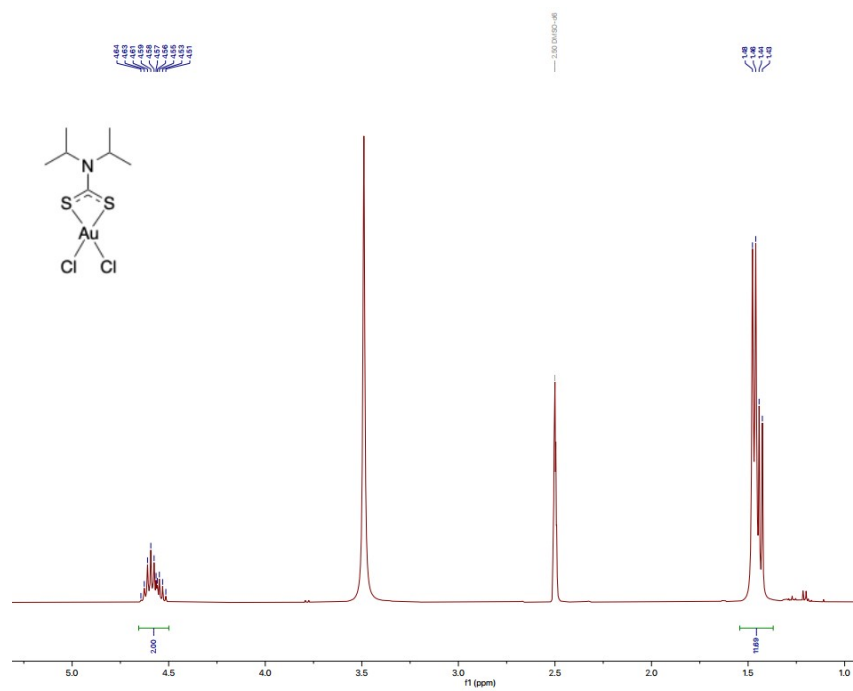


Figure S13: ^1H NMR spectrum of “[AuCl₂(*i*Pr₂dtc)]” in DMSO-d₆.

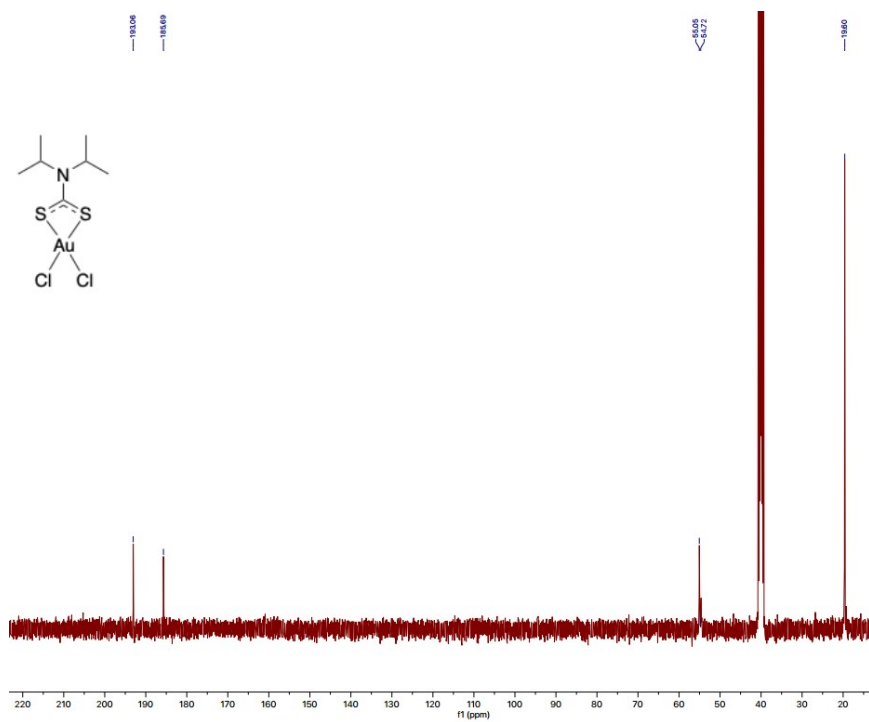


Figure S14: $^{13}\text{C}\{^1\text{H}\}$ NMR spectrum of “[AuCl₂(*i*Pr₂dtc)]” in DMSO-d₆.

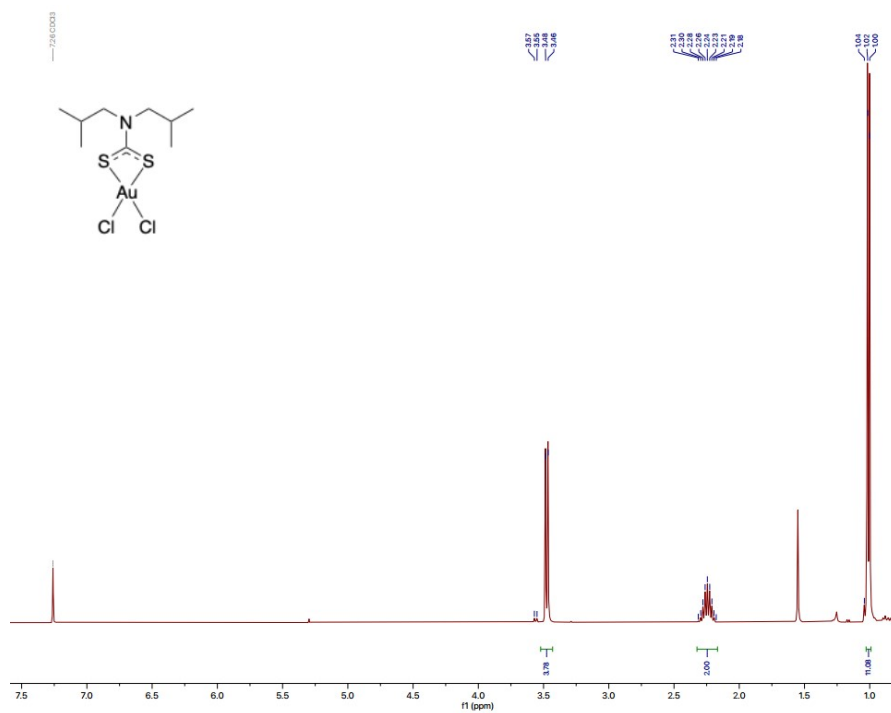


Figure S15: ^1H NMR spectrum of “[$\text{AuCl}_2(\text{iBu}_2\text{dtc})$]” in CDCl_3 .

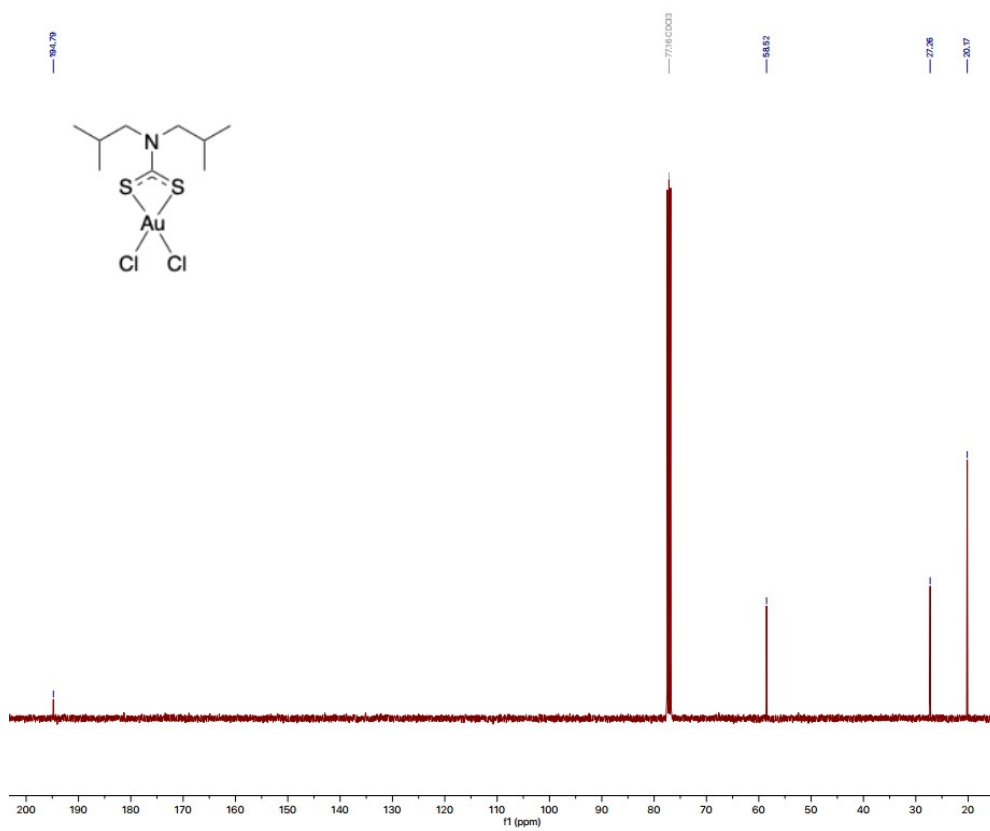


Figure S16: $^{13}\text{C}\{^1\text{H}\}$ NMR spectrum of “[$\text{AuCl}_2(\text{iBu}_2\text{dtc})$]” in CDCl_3 .

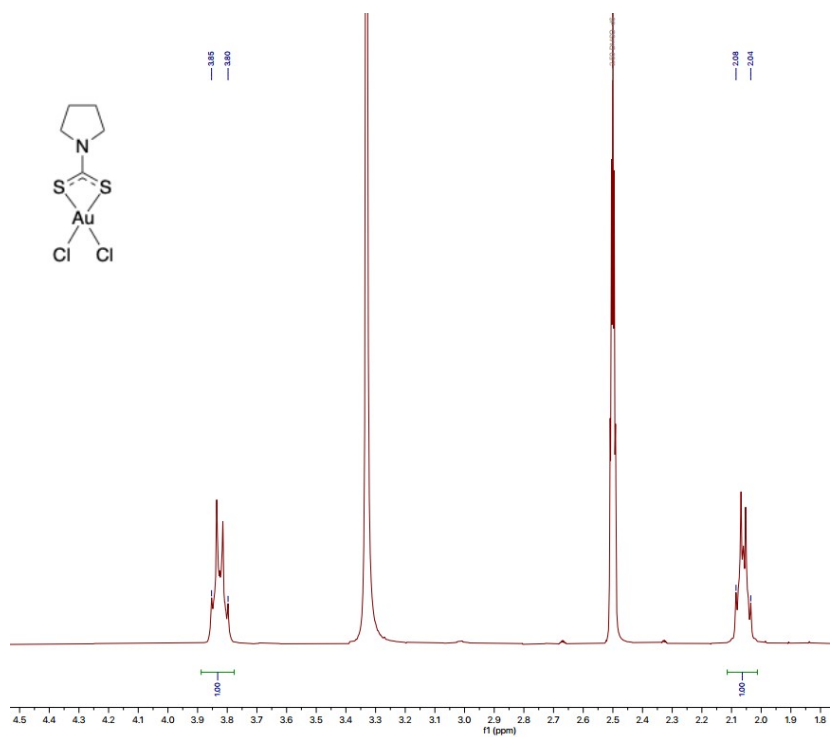


Figure S17: ^1H NMR spectrum of “[$\text{AuCl}_2(\text{pyrr-dtc})$]” in DMSO-d_6 .

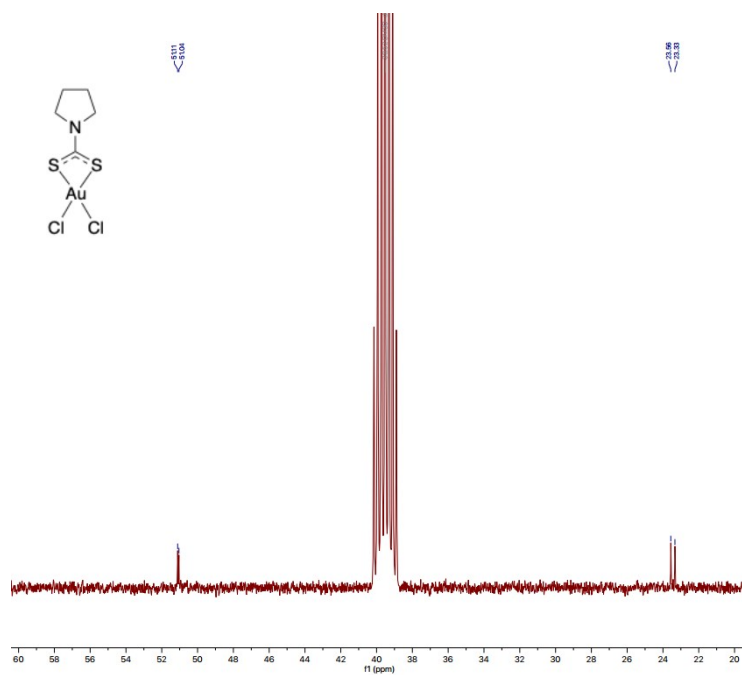


Figure S18: $^{13}\text{C}\{^1\text{H}\}$ NMR spectrum of “[$\text{AuCl}_2(\text{pyrr-dtc})$]” in DMSO-d_6 .

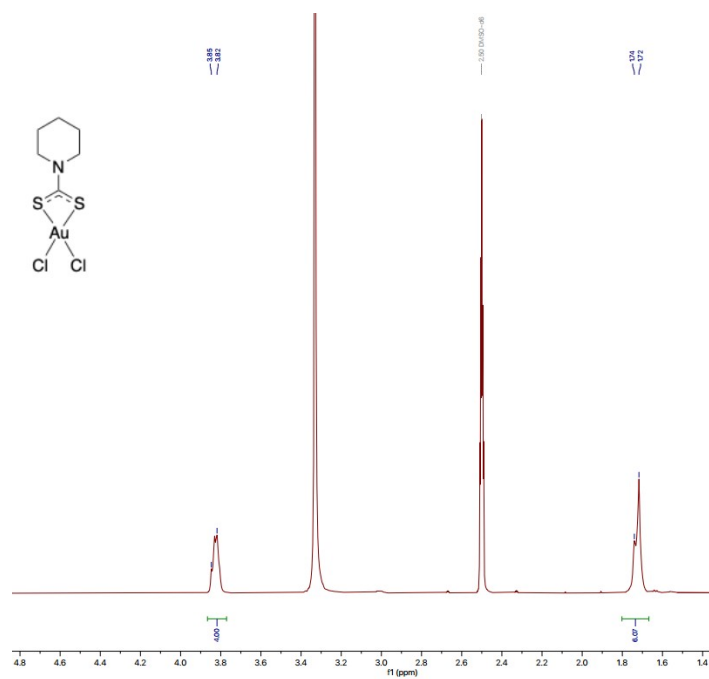


Figure S19: ^1H NMR spectrum of $[\text{AuCl}_2(\text{pip-dtc})]$ in DMSO-d_6 .

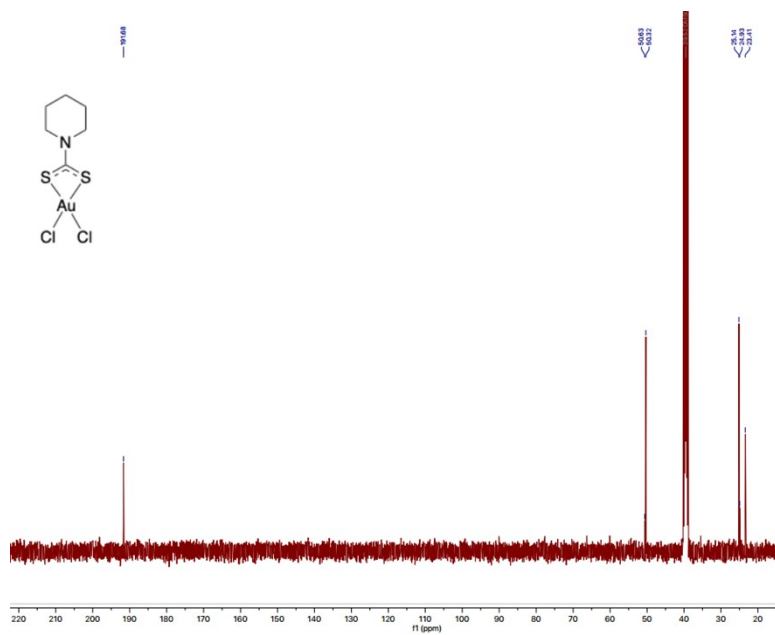


Figure S20: ^{13}C $\{^1\text{H}\}$ NMR spectrum of $[\text{AuCl}_2(\text{pip-dtc})]$ in DMSO-d_6 .

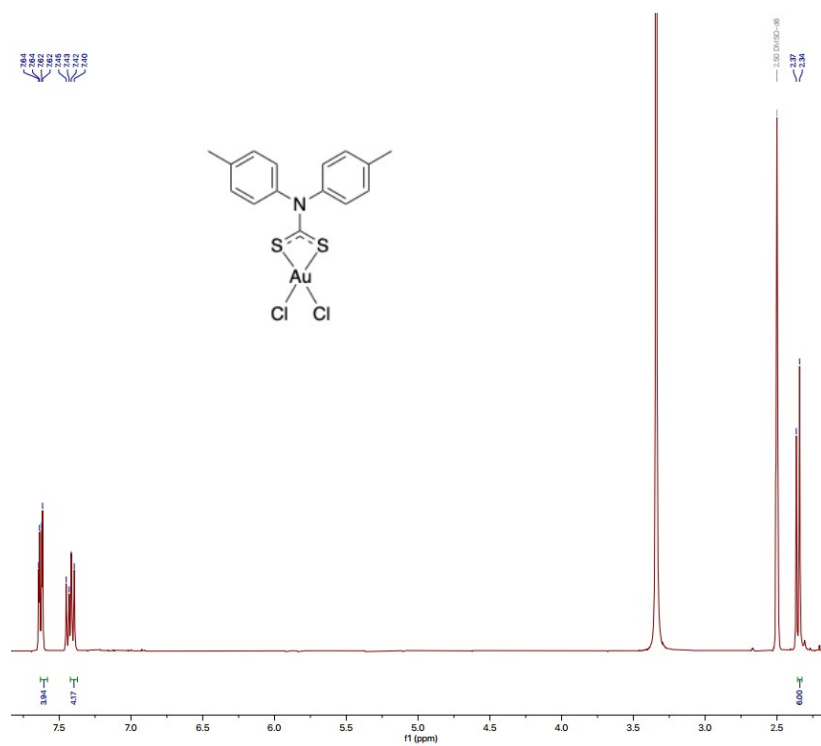


Figure S21: ^1H NMR spectrum of “[AuCl₂(p-tolyl)₂dtc]” in DMSO-d₆.

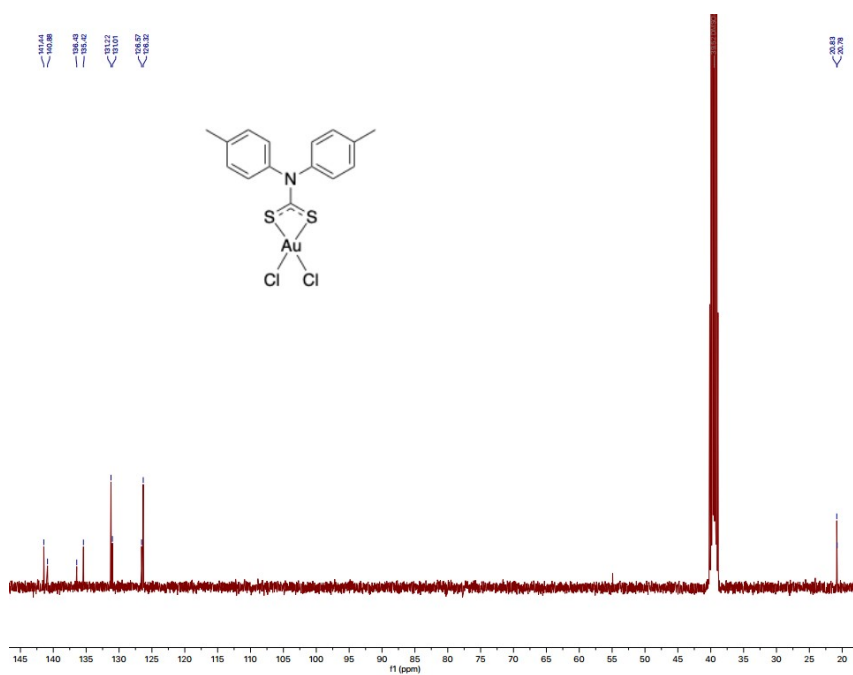


Figure S22: $^{13}\text{C}\{^1\text{H}\}$ NMR spectrum of “[AuCl₂(p-tolyl)₂dtc]” in DMSO-d₆.

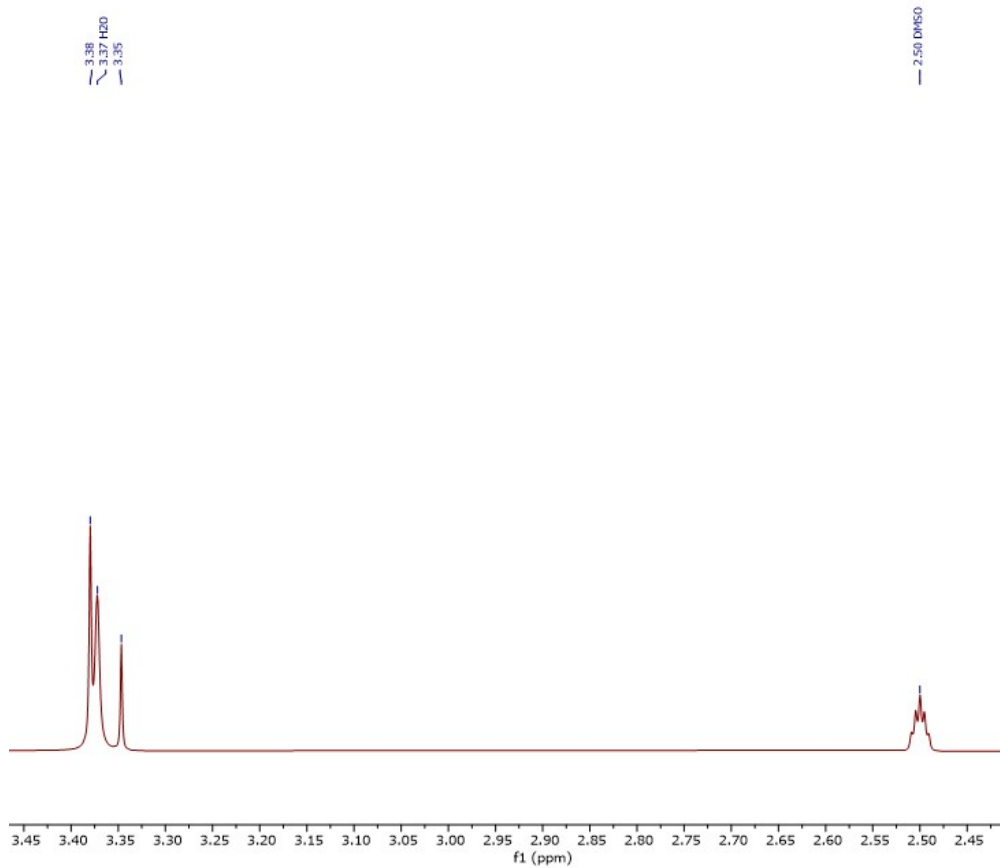


Figure S23: ^1H NMR spectrum of “[AuBr₂(Me₂dtc)]” in DMSO-d₆.

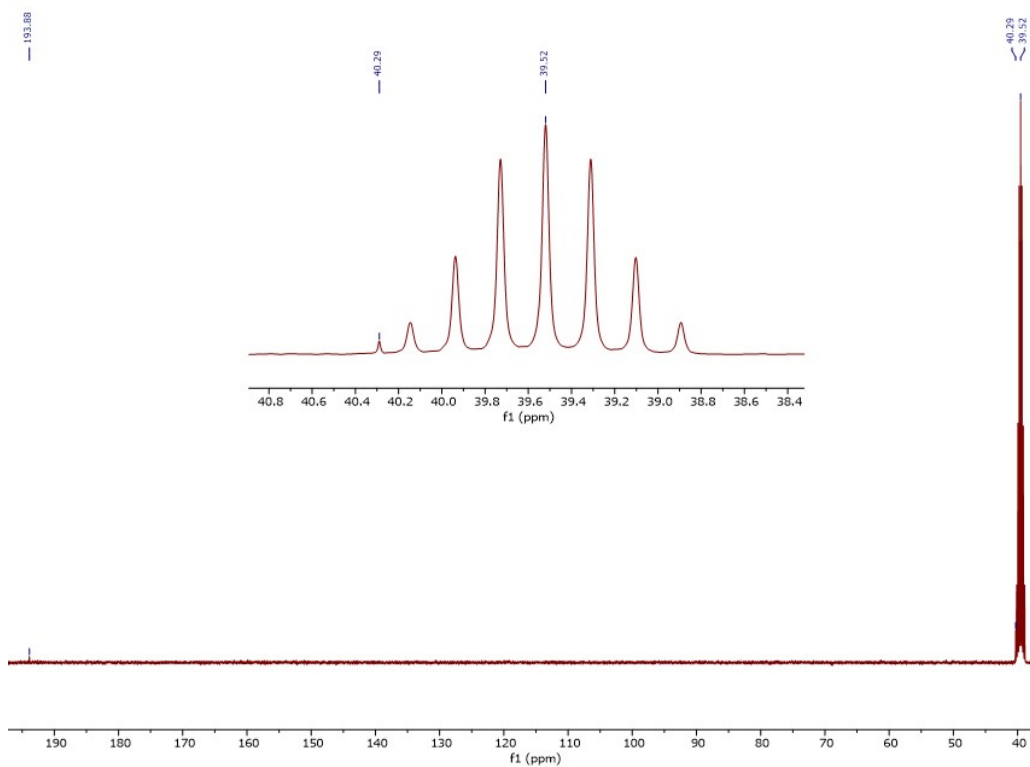


Figure S24: $^{13}\text{C}\{^1\text{H}\}$ NMR spectrum of “[AuBr₂(Me₂dtc)]” in DMSO-d₆.

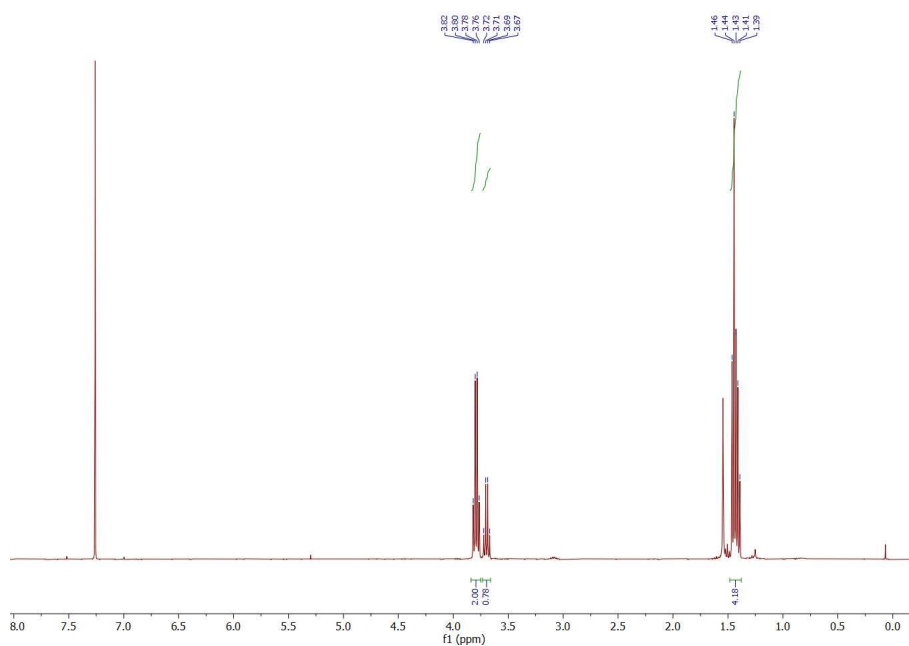


Figure S25: ^1H NMR spectrum of “[AuBr₂(Et₂dtc)]” in CDCl₃.

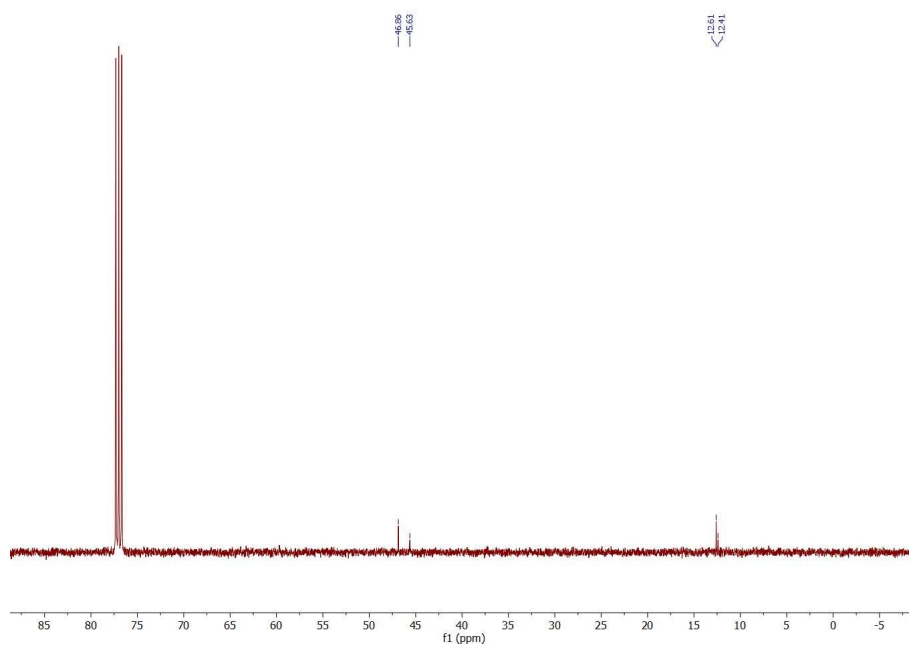


Figure S26: $^{13}\text{C}\{^1\text{H}\}$ NMR spectrum of “[AuBr₂(Et₂dtc)]” in CDCl₃.

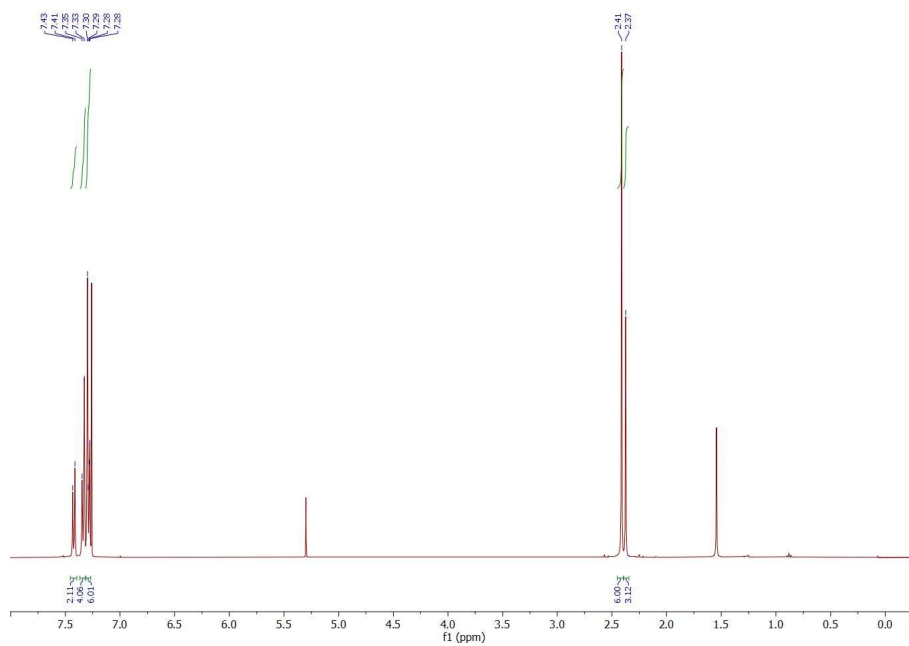


Figure S27: ^1H NMR spectrum of “[AuBr₂(p-tolyl₂dtc)]” in CDCl₃.

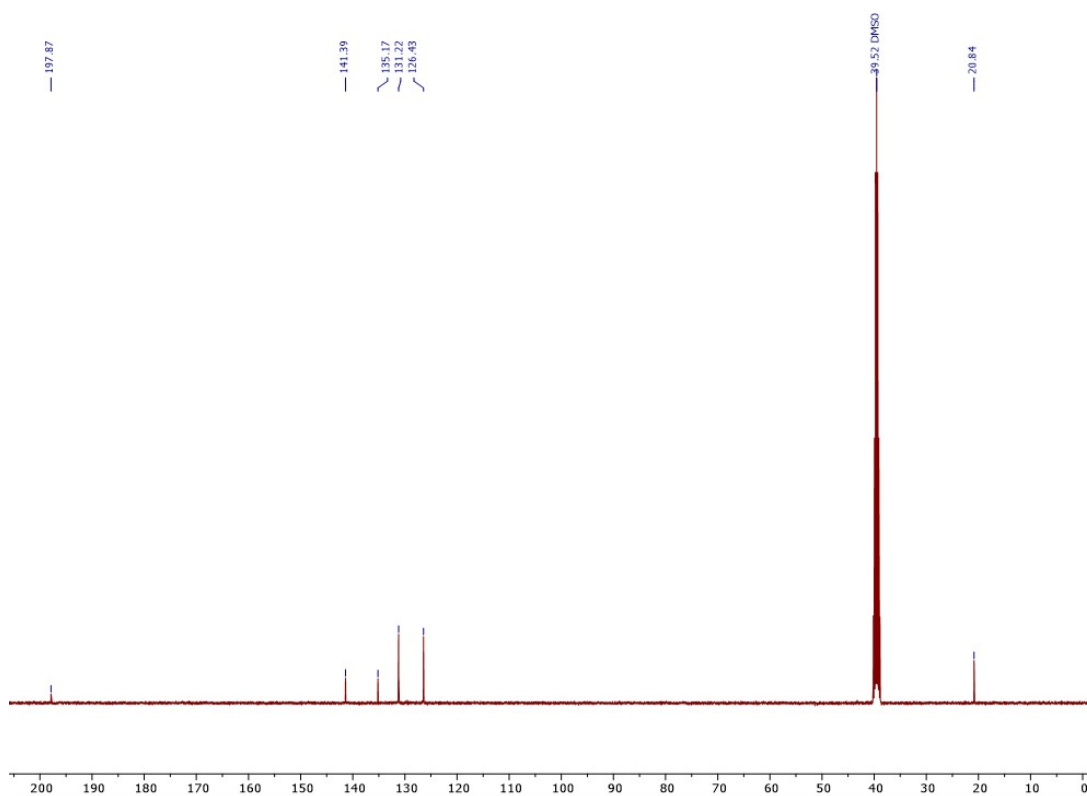


Figure S28: $^{13}\text{C}\{^1\text{H}\}$ NMR spectrum of “[AuBr₂(p-tolyl₂dtc)]” in CDCl₃.

3.2 NMR spectra of analytically pure compounds

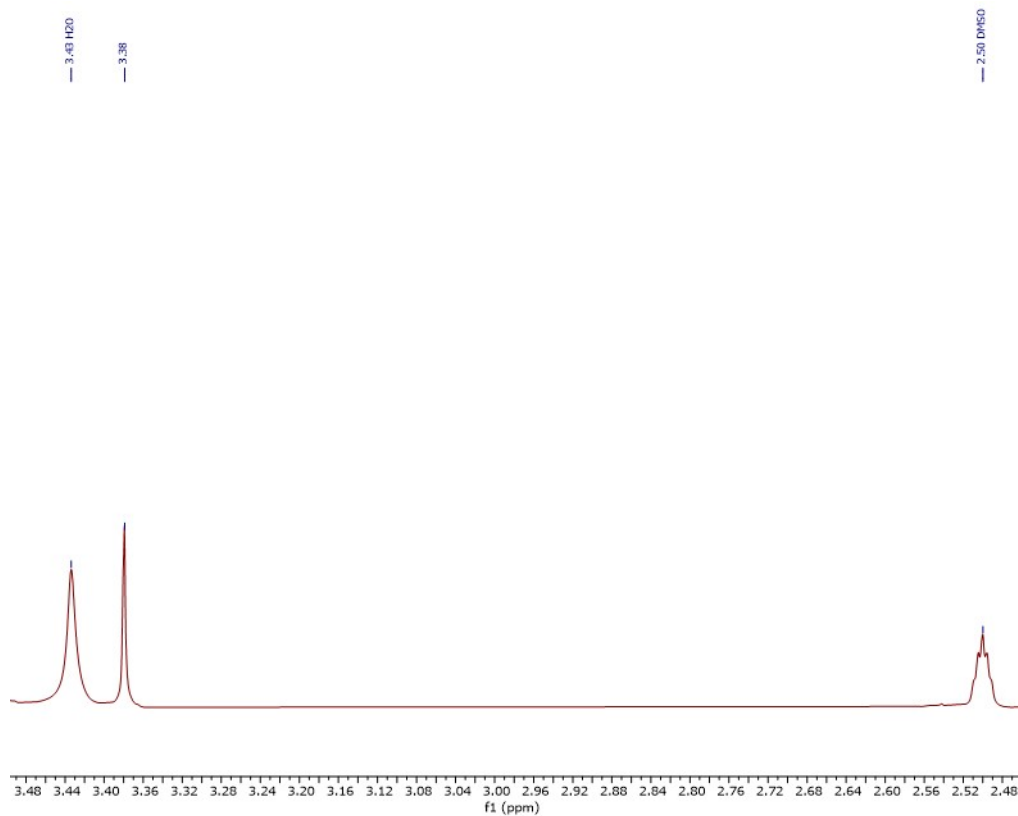


Figure S29: ^1H NMR spectrum of pure $[\text{AuCl}_2(\text{Me}_2\text{dtc})]$ in DMSO-d_6 .

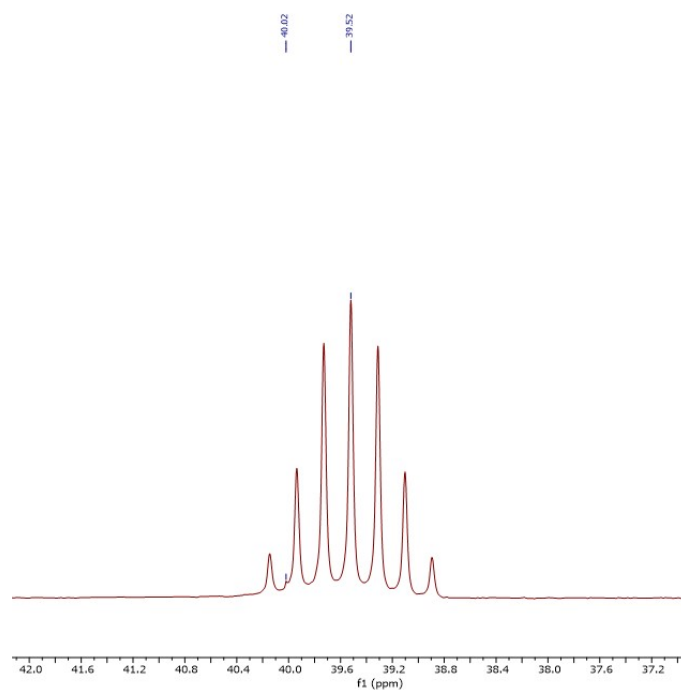


Figure S30: $^{13}\text{C}\{^1\text{H}\}$ NMR spectrum of pure $[\text{AuCl}_2(\text{Me}_2\text{dtc})]$ in DMSO-d_6 .

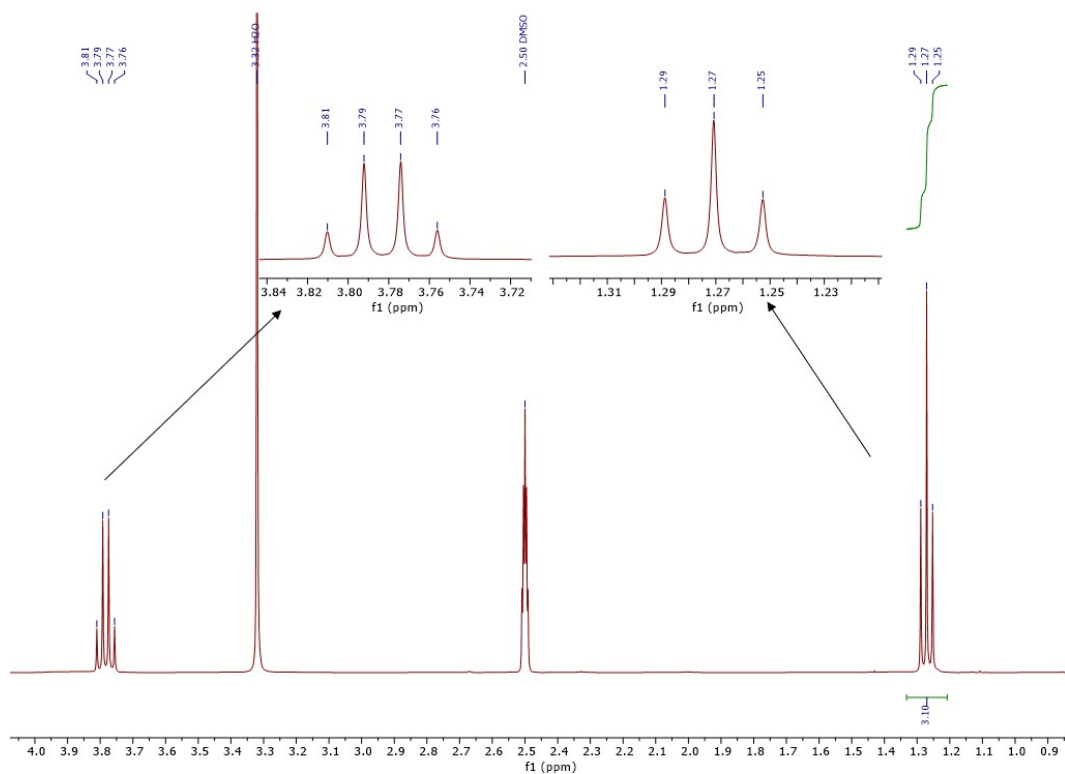


Figure S31: ^1H NMR spectrum of pure $[\text{AuCl}_2(\text{Et}_2\text{dtc})]$ in DMSO-d_6 .

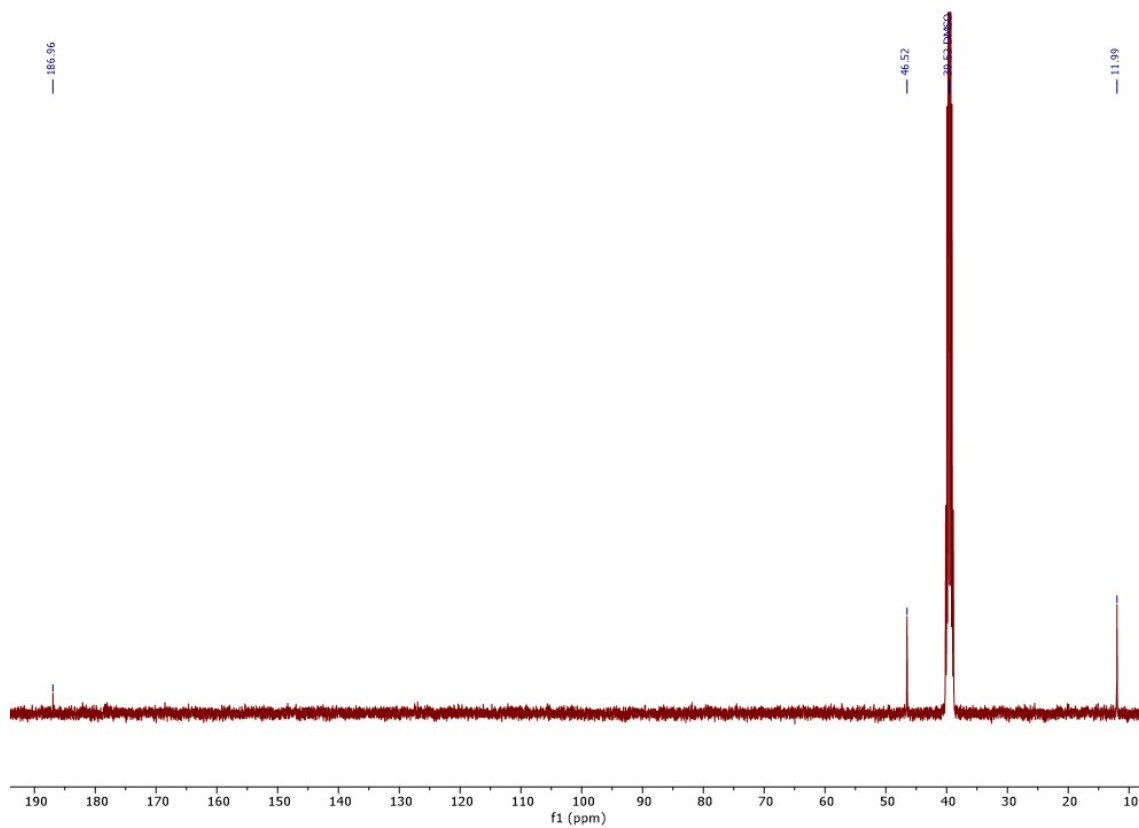


Figure S32: $^{13}\text{C}\{^1\text{H}\}$ NMR spectrum of pure $[\text{AuCl}_2(\text{Et}_2\text{dtc})]$ in DMSO-d_6 .

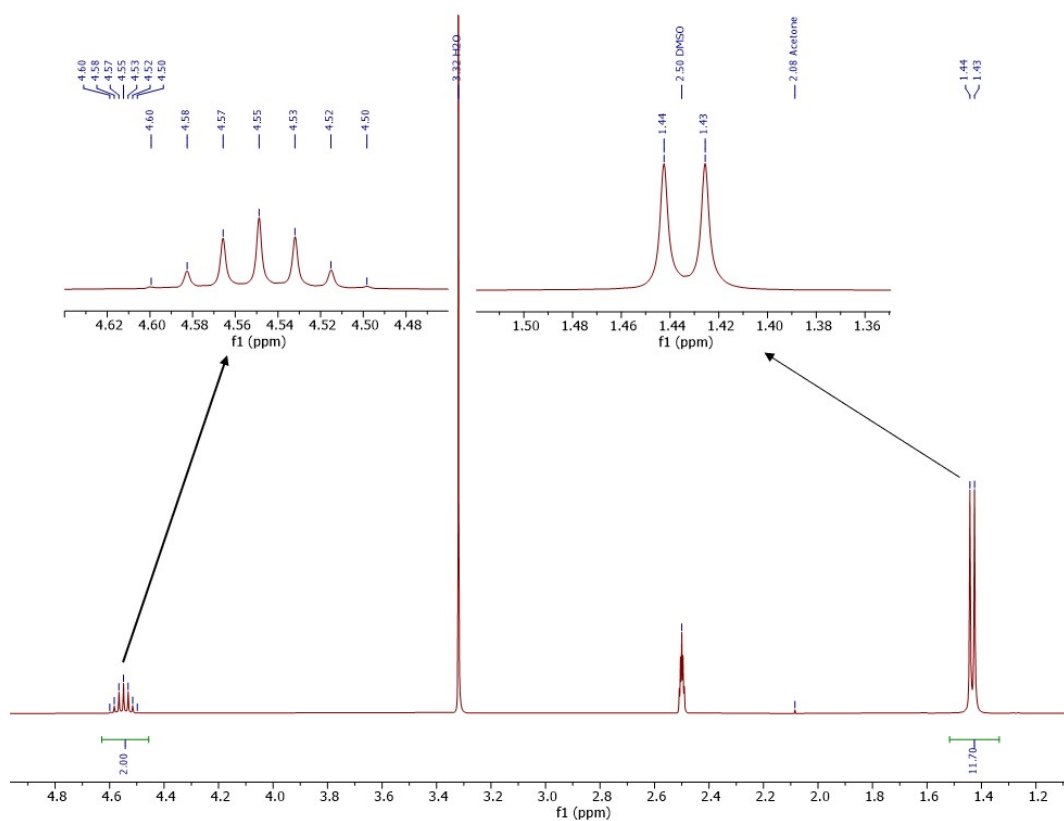


Figure S33: ^1H NMR spectrum of pure $[\text{AuCl}_2(\text{iPr}_2\text{dtc})]$ in DMSO-d_6 .

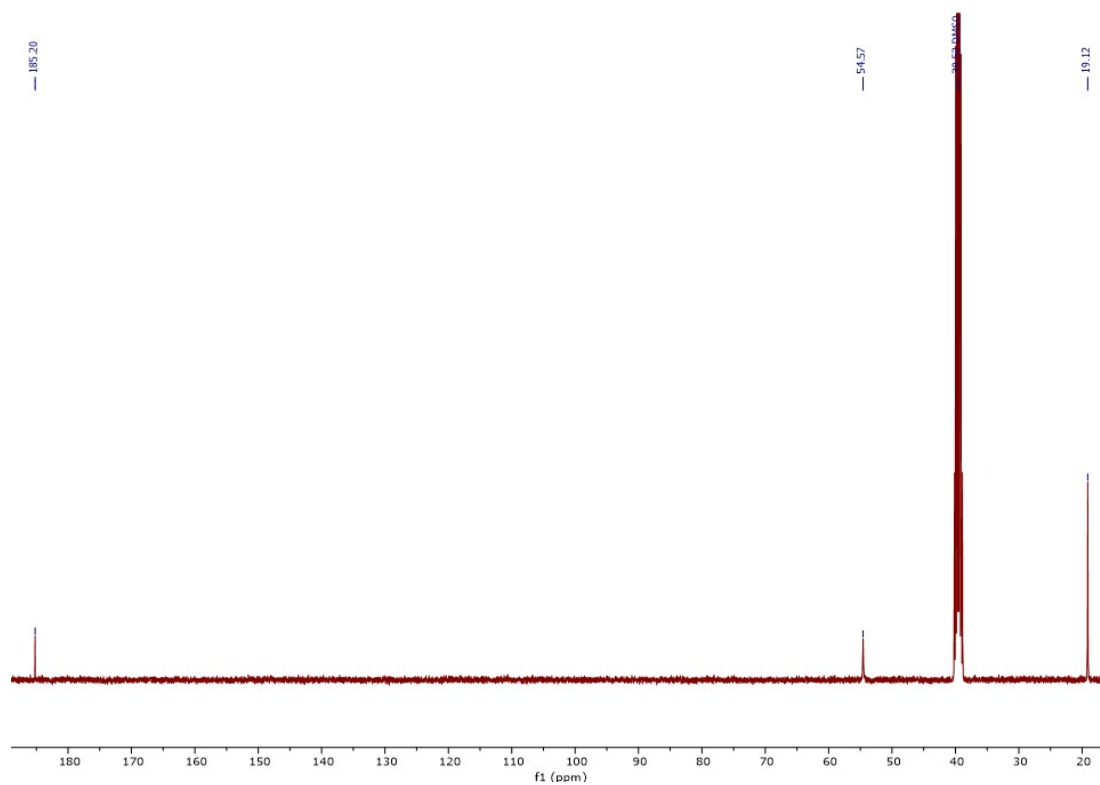


Figure S34: $^{13}\text{C}\{^1\text{H}\}$ NMR spectrum of pure $[\text{AuCl}_2(\text{iPr}_2\text{dtc})]$ in DMSO-d_6 .

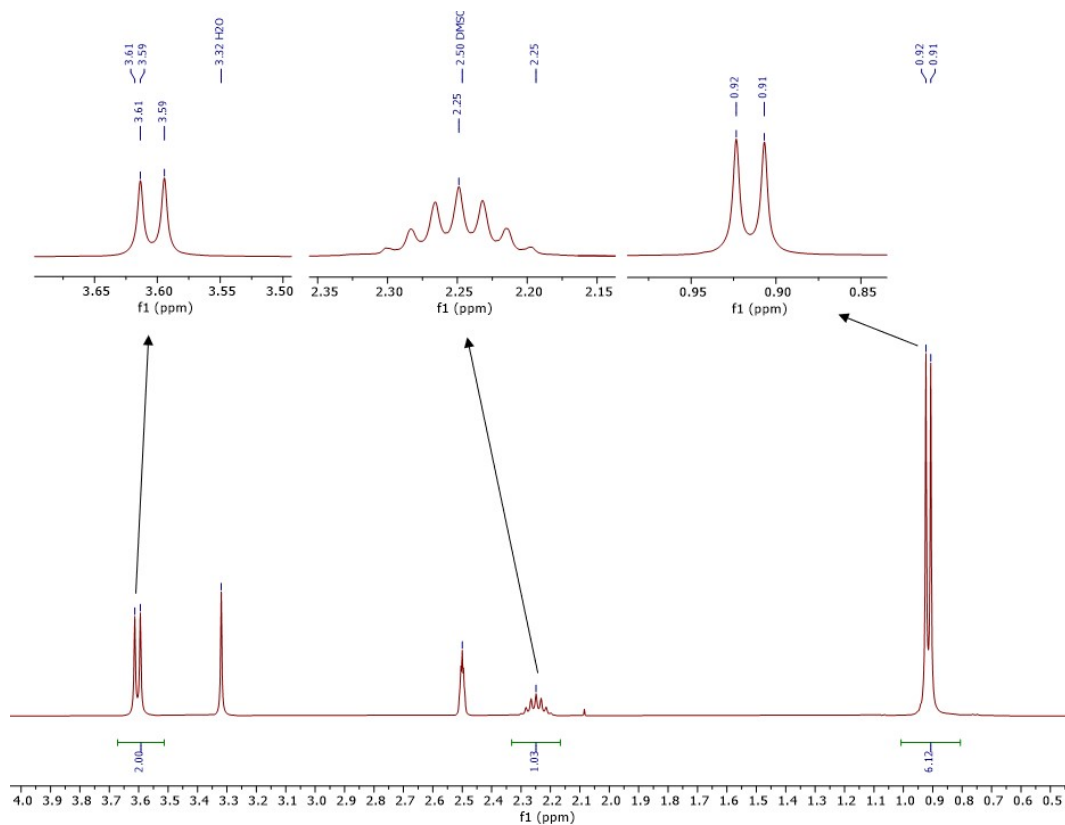


Figure S35: ^1H NMR spectrum of pure $[\text{AuCl}_2(\textit{i}\text{Bu}_2\text{dtc})]$ in DMSO-d_6 .

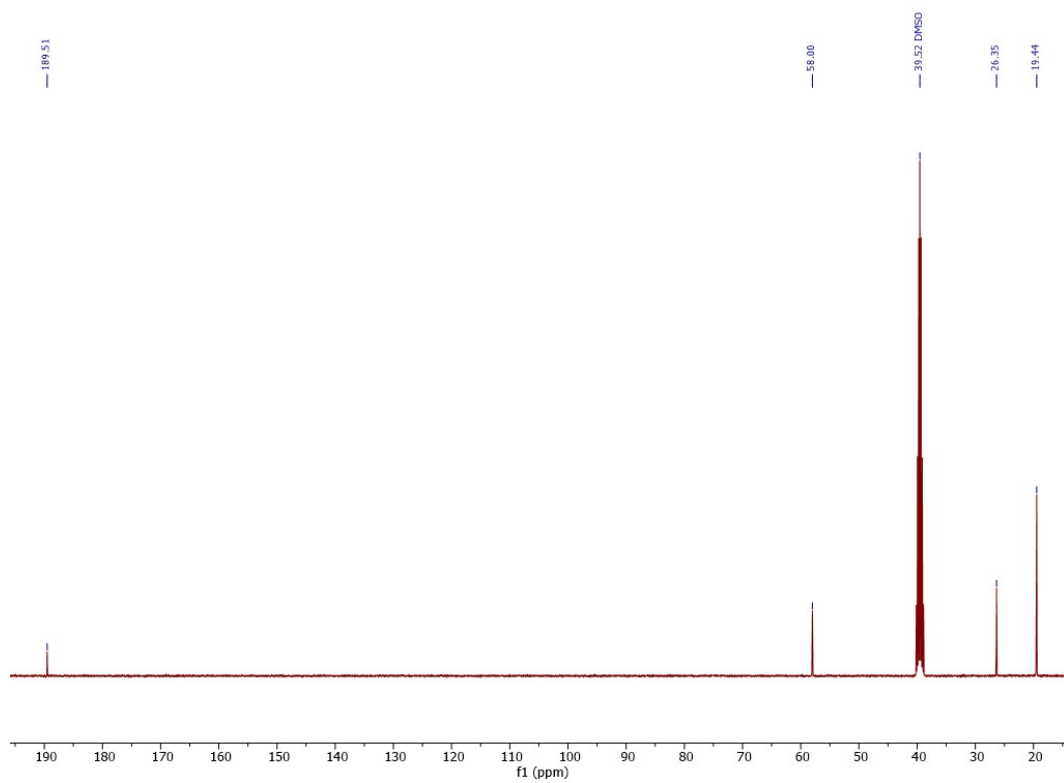


Figure S36: $^{13}\text{C}\{^1\text{H}\}$ NMR spectrum of pure $[\text{AuCl}_2(\textit{i}\text{Bu}_2\text{dtc})]$ in DMSO-d_6 .

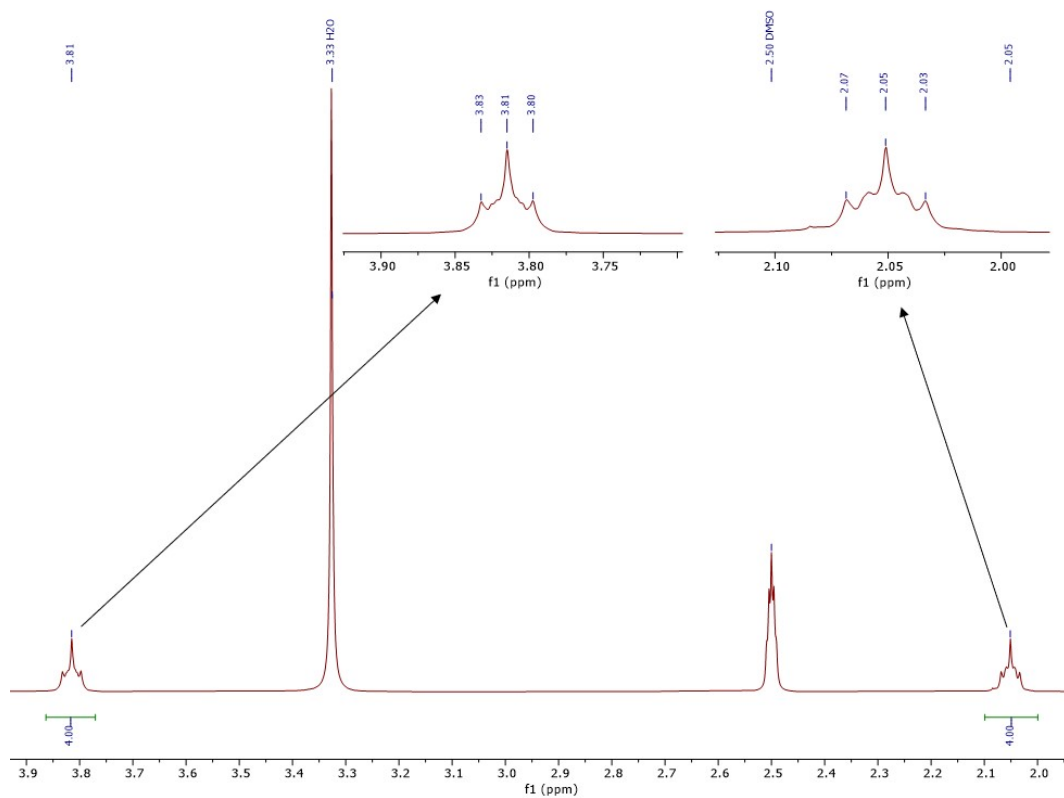


Figure S37: ^1H NMR spectrum of pure $[\text{AuCl}_2(\text{pyrr-dtc})]$ in DMSO-d_6 .

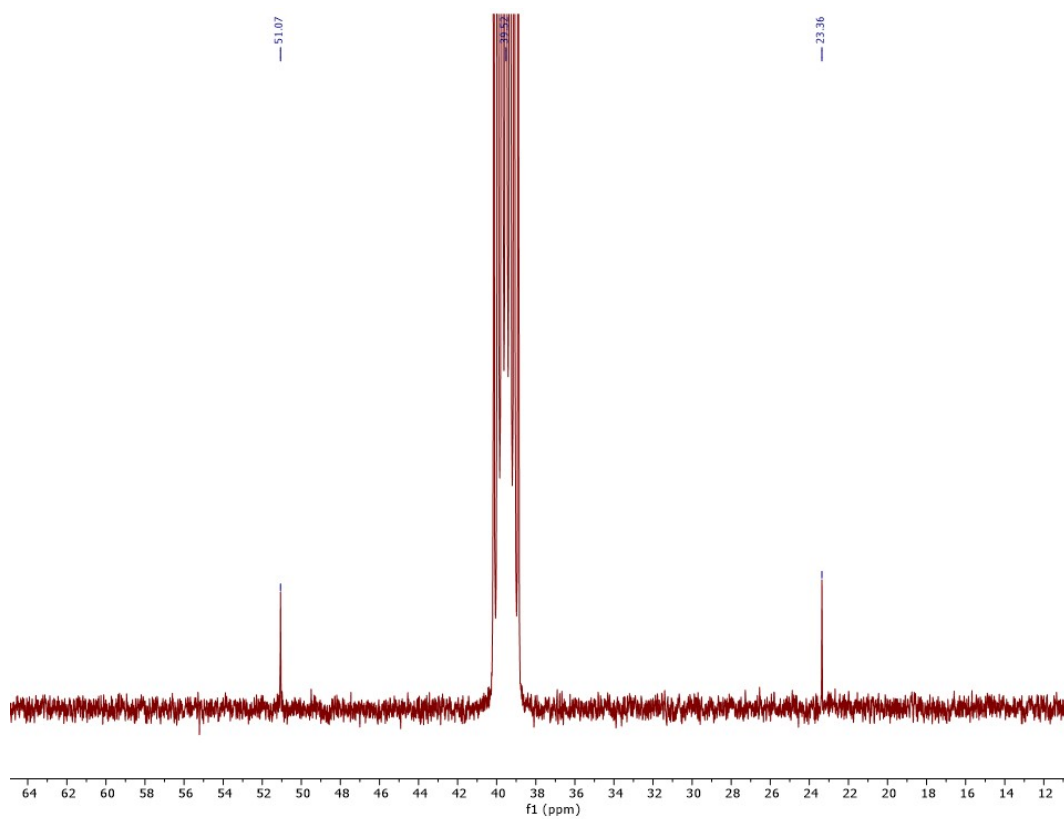


Figure S38: $^{13}\text{C}\{^1\text{H}\}$ NMR spectrum of pure $[\text{AuCl}_2(\text{pyrr-dtc})]$ in DMSO-d_6 .

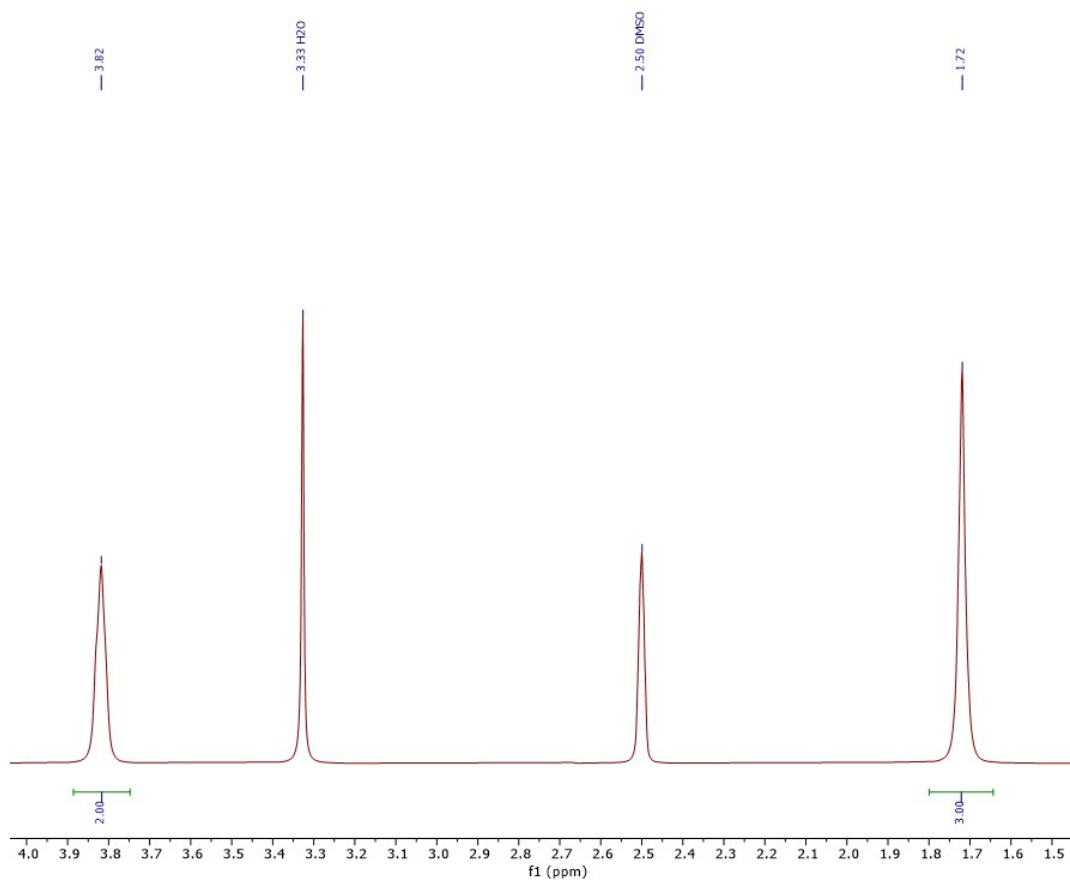


Figure S39: ^1H NMR spectrum of pure $[\text{AuCl}_2(\text{pip-dtc})]$ in DMSO-d_6 .

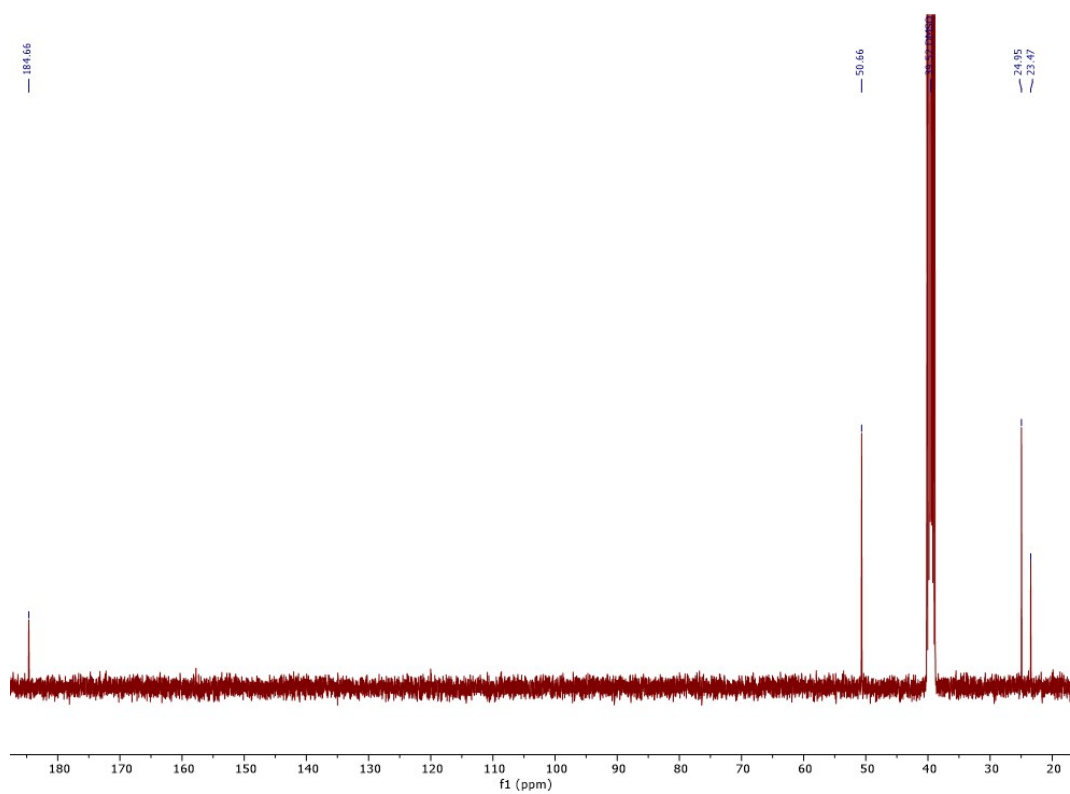


Figure S40: $^{13}\text{C}\{^1\text{H}\}$ NMR spectrum of pure $[\text{AuCl}_2(\text{pip-dtc})]$ in DMSO-d_6 .

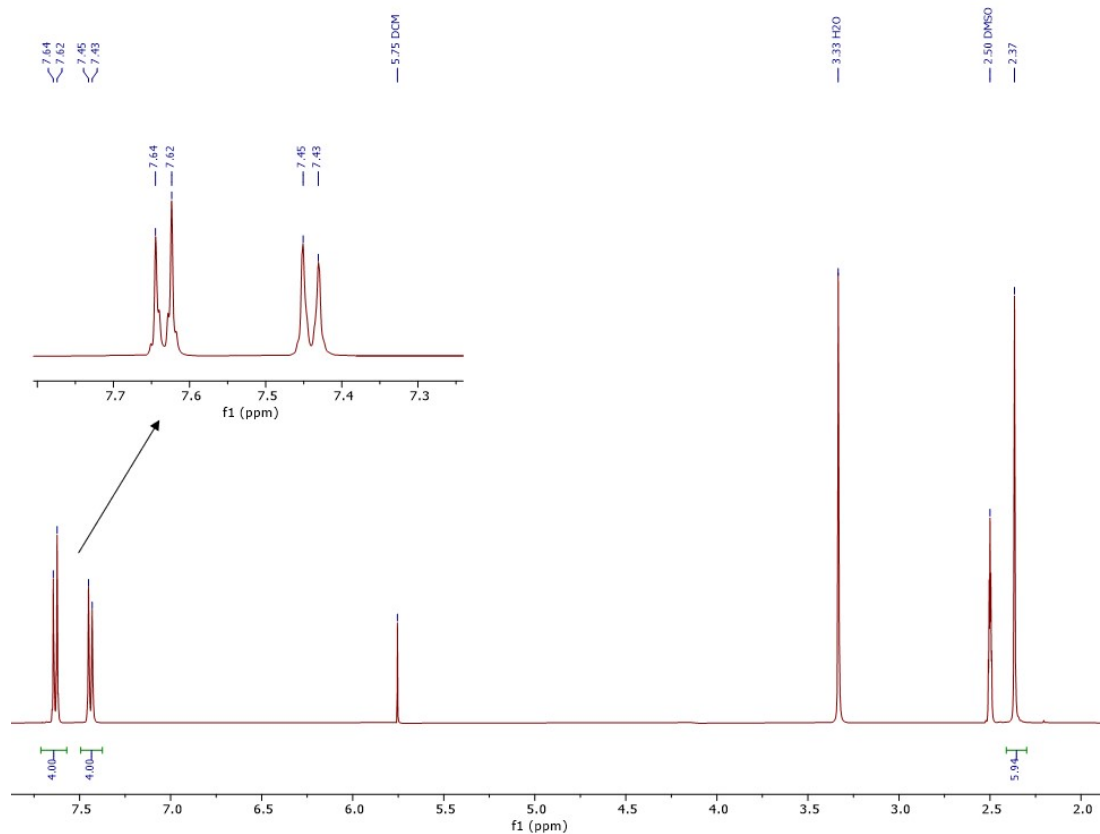


Figure S41: ^1H NMR spectrum of pure $[\text{AuCl}_2(\text{p-tolyl})_2\text{dtc}]$ in DMSO-d_6 .

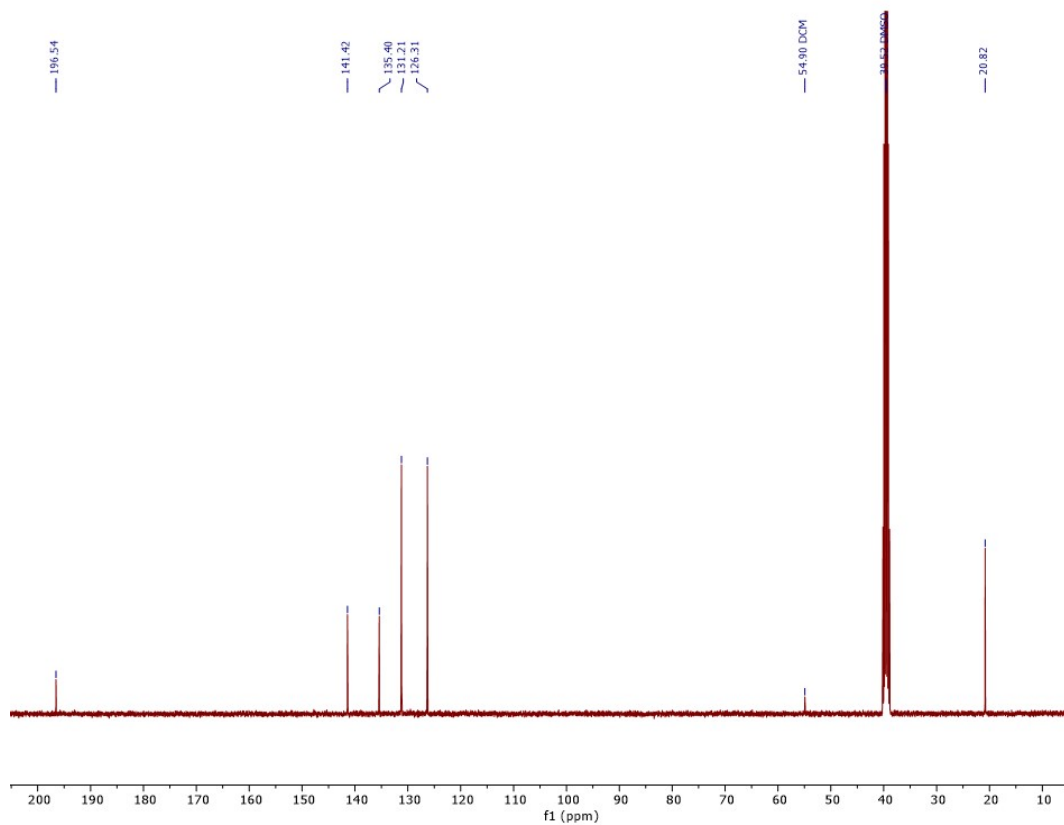


Figure S42: $^{13}\text{C}\{^1\text{H}\}$ NMR spectrum of pure $[\text{AuCl}_2(\text{p-tolyl})_2\text{dtc}]$ in DMSO-d_6 .

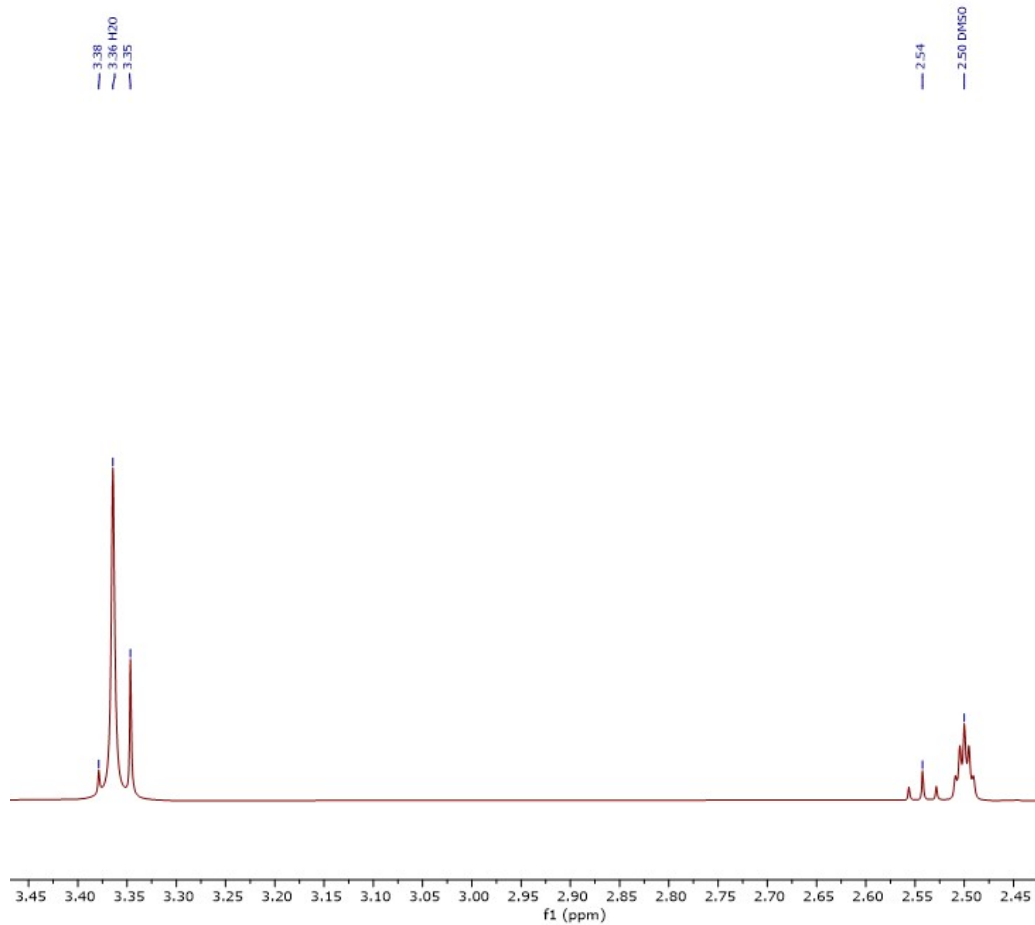


Figure S43: ^1H NMR spectrum of pure $[\text{AuBr}_2(\text{Me}_2\text{dtc})]$ in DMSO-d_6 .

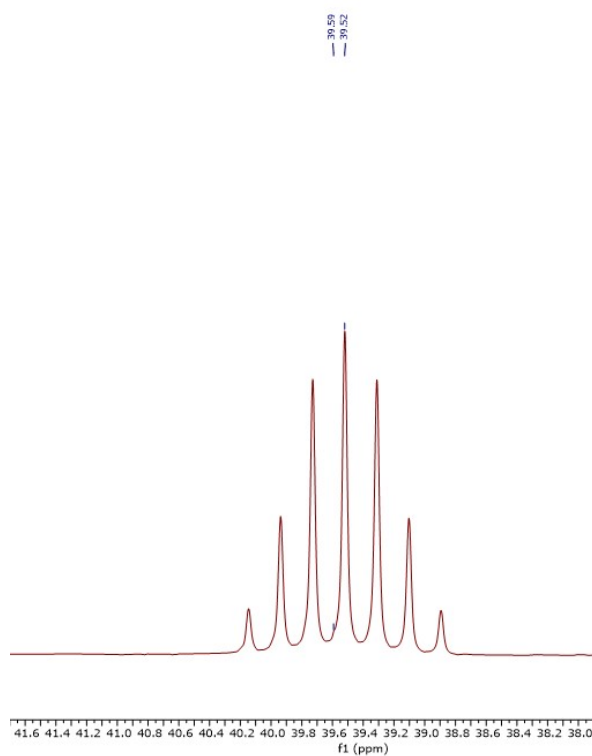


Figure S44: $^{13}\text{C}\{^1\text{H}\}$ NMR spectrum of pure $[\text{AuBr}_2(\text{Me}_2\text{dtc})]$ in DMSO-d_6 .

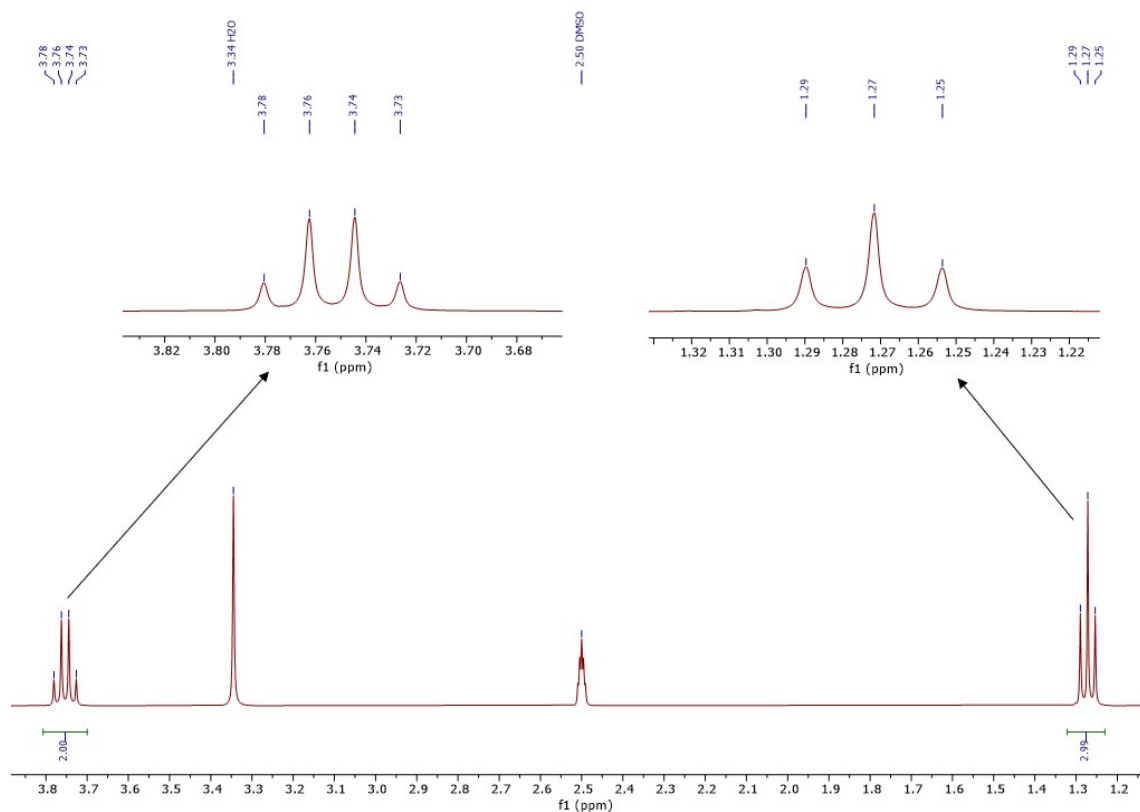


Figure S45: ^1H NMR spectrum of pure $[\text{AuBr}_2(\text{Et}_2\text{dtc})]$ in DMSO-d_6 .

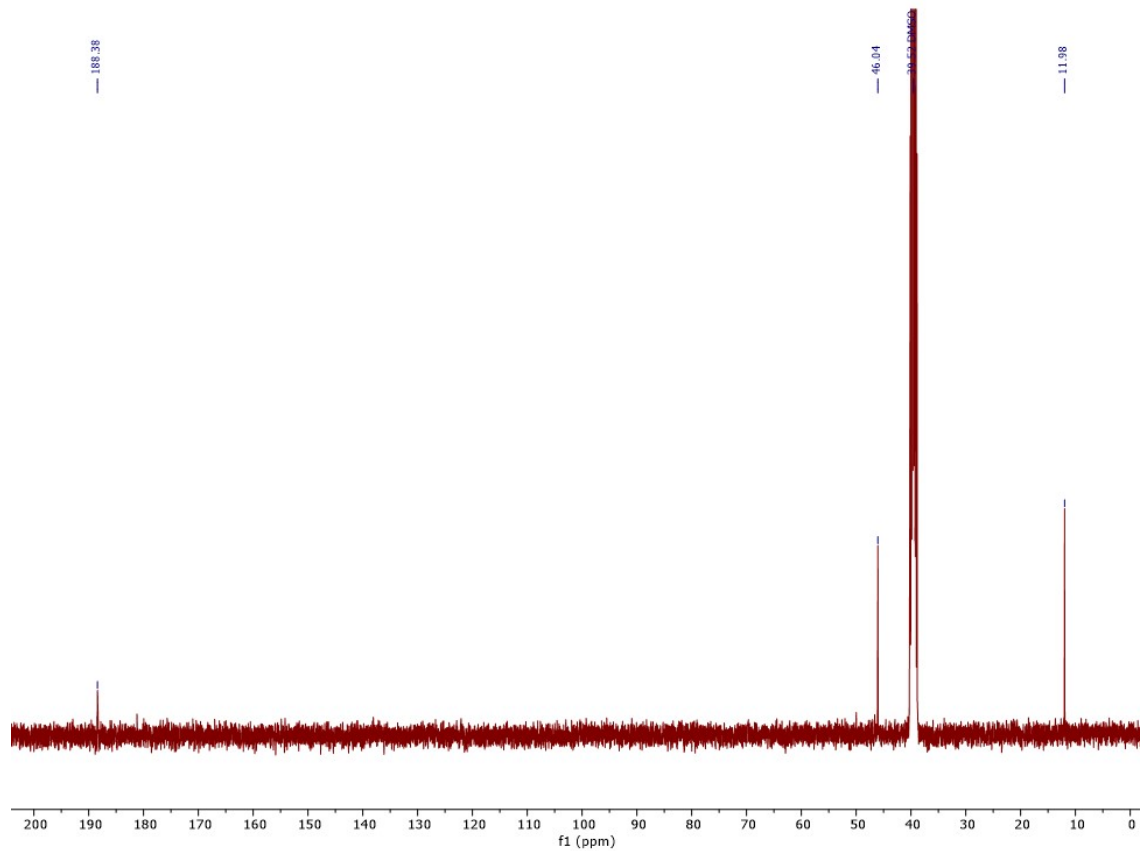
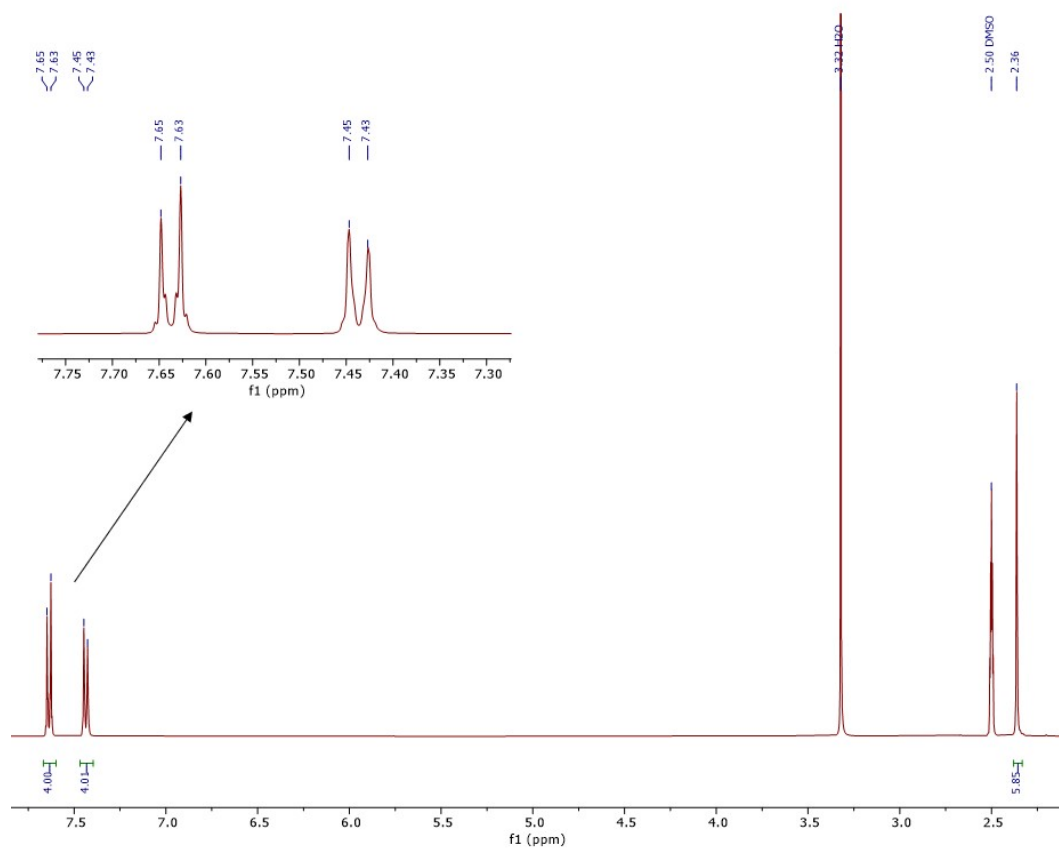


Figure S46: $^{13}\text{C}\{^1\text{H}\}$ NMR spectrum of pure $[\text{AuBr}_2(\text{Et}_2\text{dtc})]$ in DMSO-d_6 .



re S47: ^1H NMR spectrum of pure $[\text{AuBr}_2(\text{p-tolyl})_2\text{dtc}]$ in DMSO-d_6 .

Fig

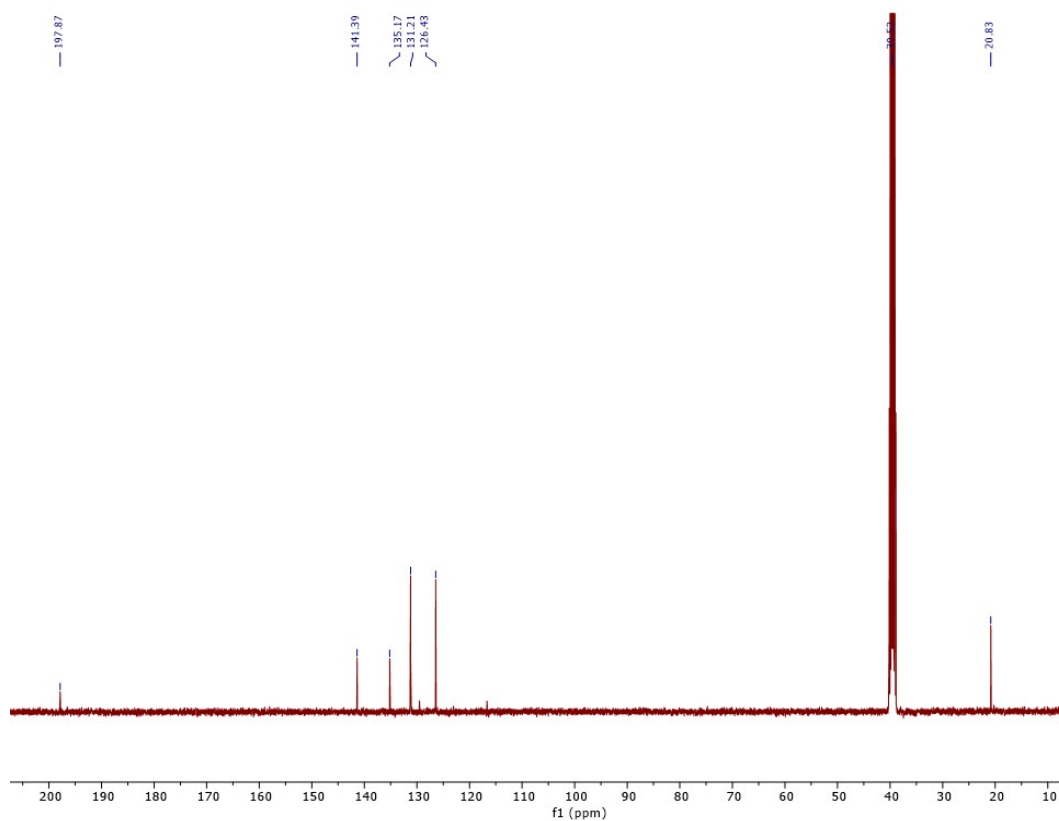


Figure S48: $^{13}\text{C}\{^1\text{H}\}$ NMR spectrum of pure $[\text{AuBr}_2(\text{p-tolyl})_2\text{dtc}]$ in DMSO-d_6 .

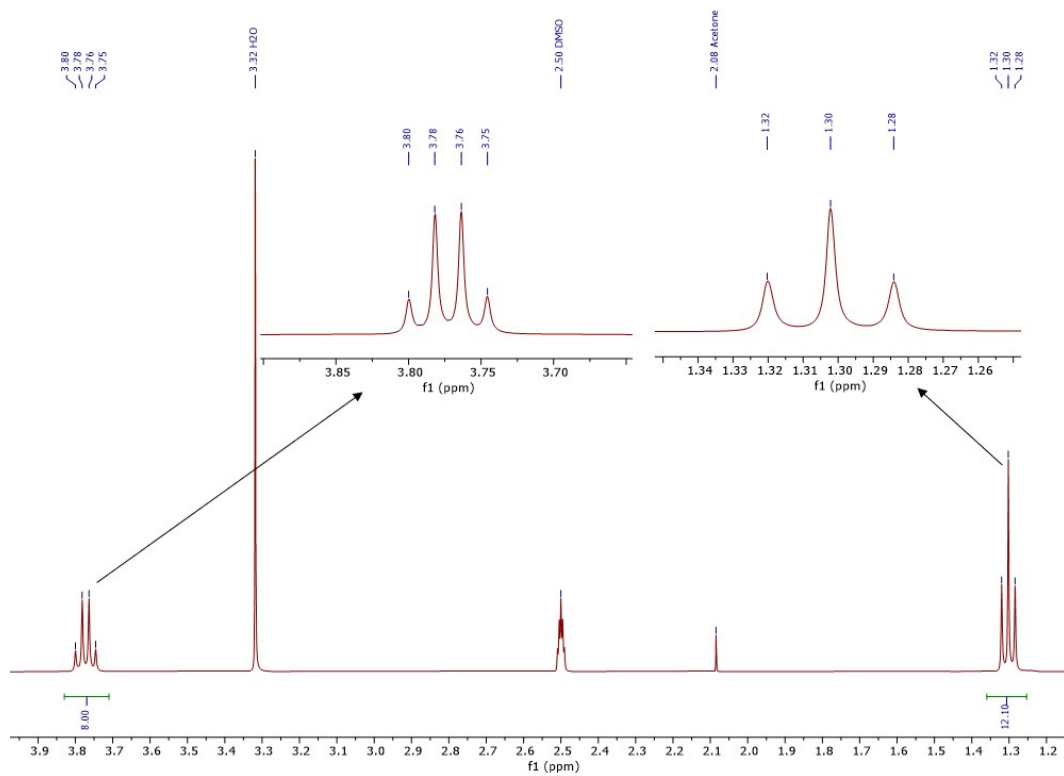


Figure S49: ^1H NMR spectrum of pure $[\text{Au}(\text{Et}_2\text{dtc})_2][\text{BF}_4]$ in DMSO-d_6 .

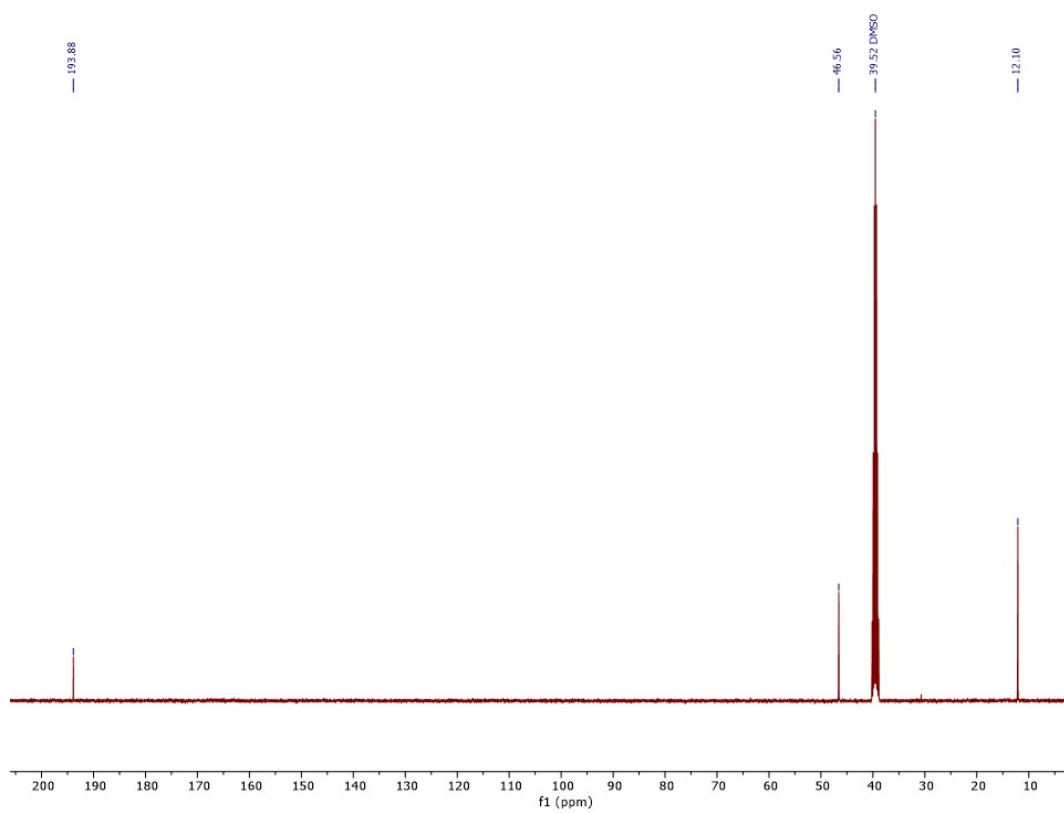


Figure S50: $^{13}\text{C}\{^1\text{H}\}$ NMR spectrum of pure $[\text{Au}(\text{Et}_2\text{dtc})_2][\text{BF}_4]$ in DMSO-d_6 .

4.3 Additional NMR spectra from investigations into the mixtures

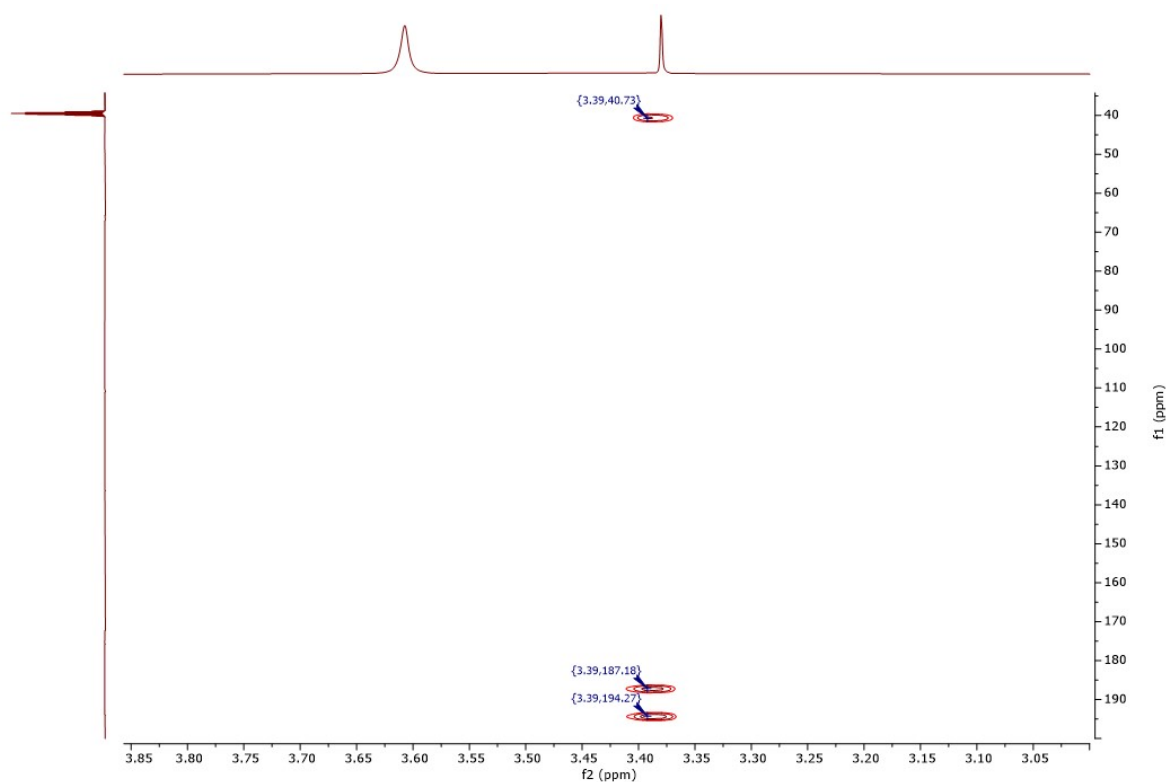


Figure S51: HMBC NMR spectrum of the “[AuCl₂(Me₂dtc)]” mixture in DMSO-d₆. This shows the presence of two distinct dithiocarbamate carbon centres which both couple to the CH₃ protons, which otherwise cannot be seen due to the low solubility of [AuCl₂(Me₂dtc)]

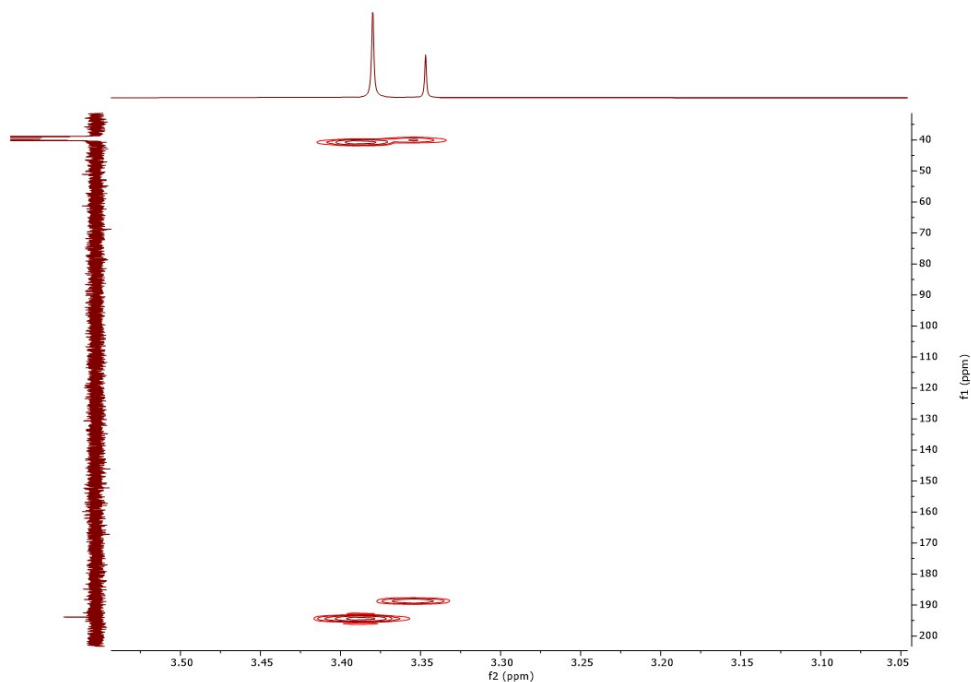


Figure S52: HMBC NMR spectrum of the “[AuCl₂(Et₂dtc)]” mixture in DMSO-d₆, also showing two distinct dithiocarbamate carbon centres which otherwise cannot be seen.

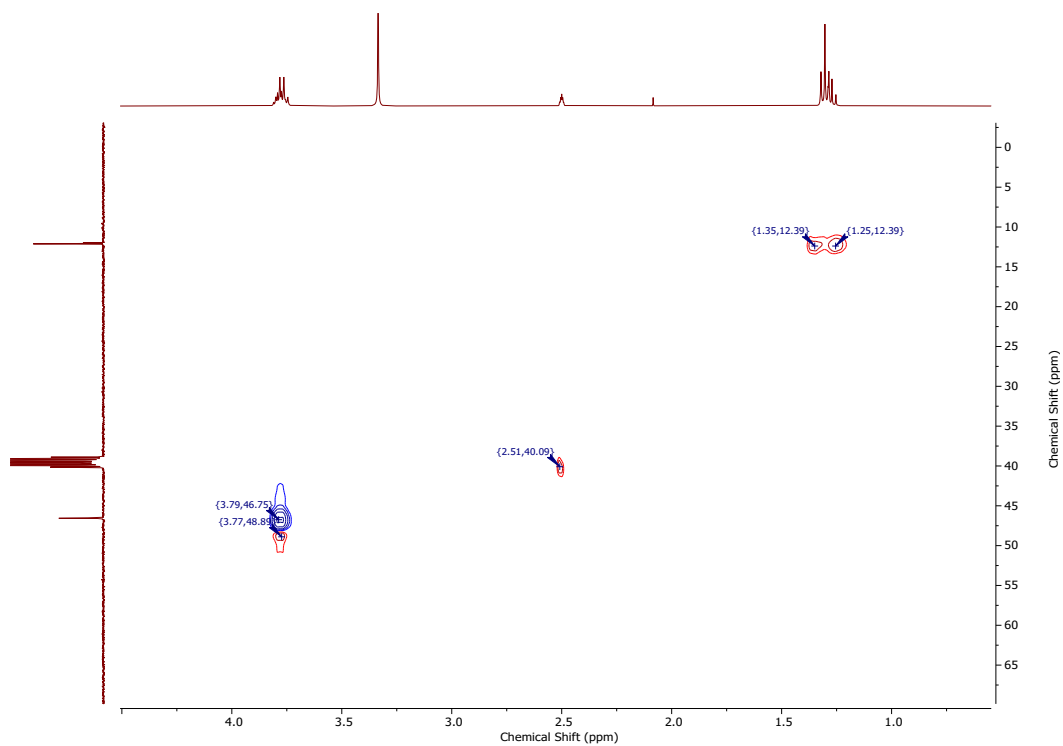


Figure S53: HSQC NMR spectrum of $[\text{AuCl}_2(\text{Et}_2\text{dtc})]/[\text{Au}(\text{Et}_2\text{dtc})_2]/[\text{AuCl}_4]$ in DMSO-d_6 .

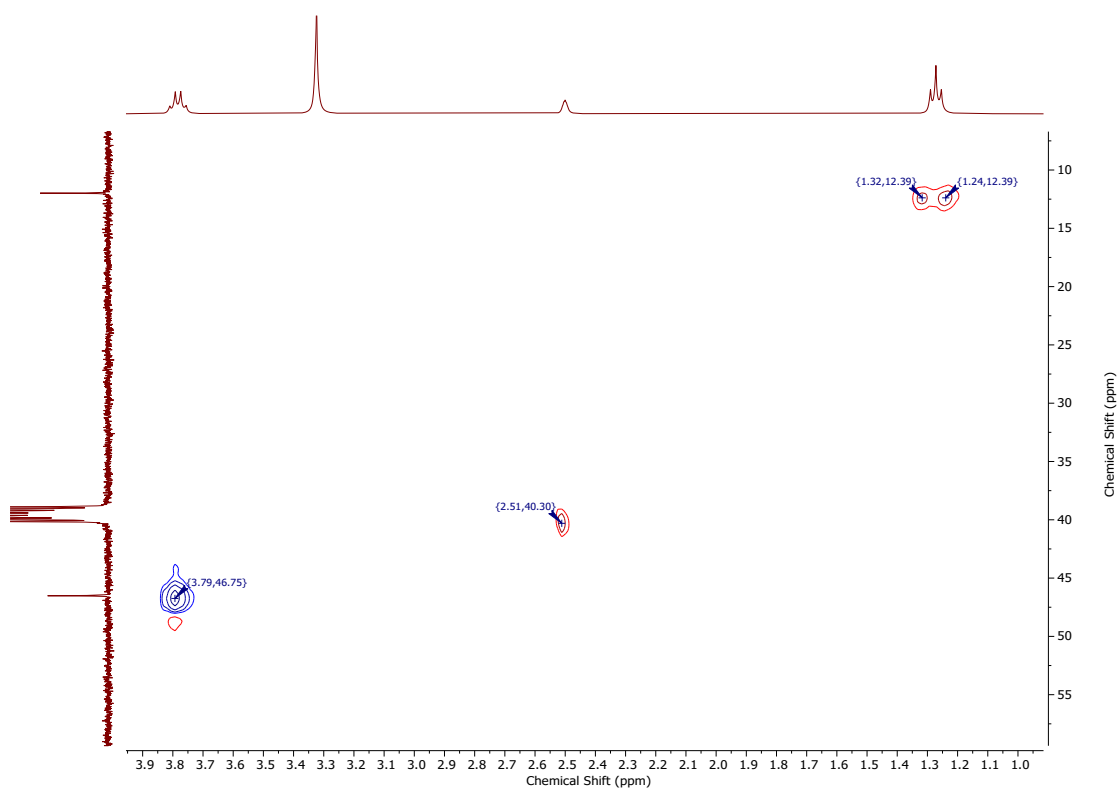


Figure S54: HSQC NMR spectrum of $[\text{AuCl}_2(\text{Et}_2\text{dtc})]$ in DMSO-d_6 .

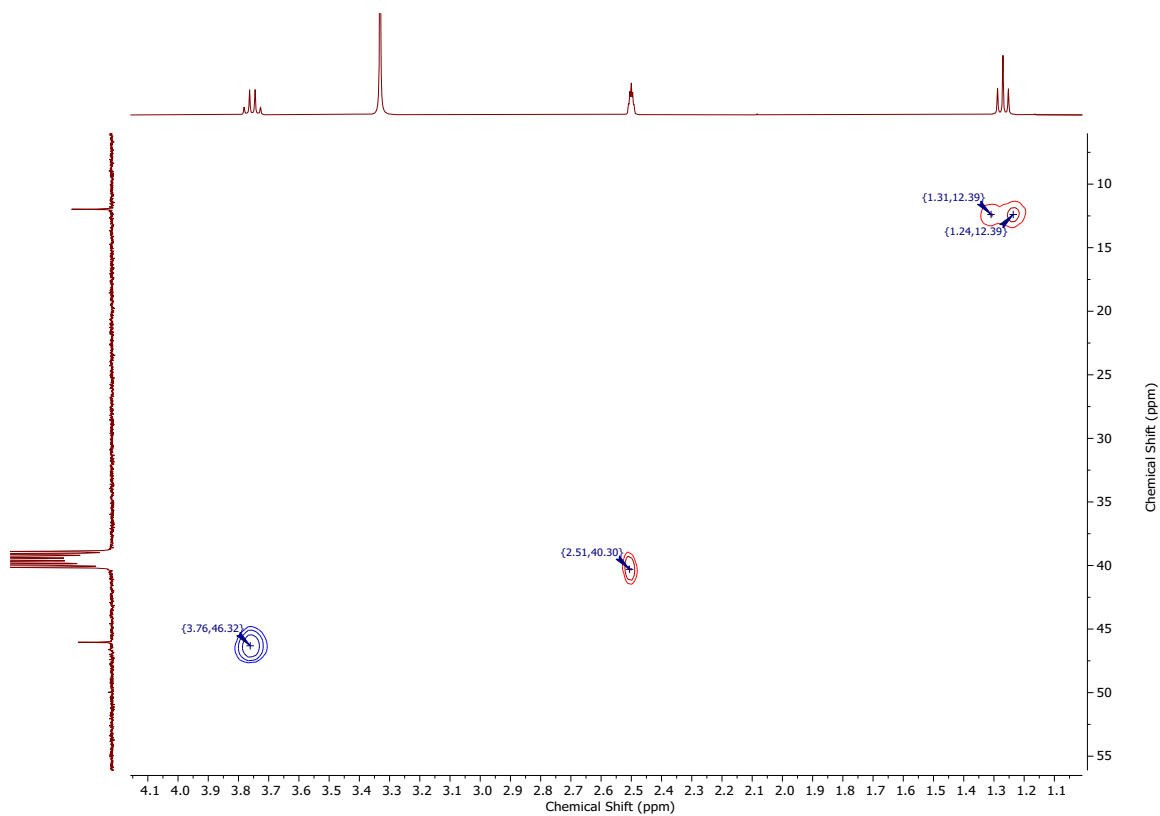


Figure S55: HSQC NMR spectrum of $[\text{AuBr}_2(\text{Et}_2\text{dtc})]$ in DMSO-d_6 .

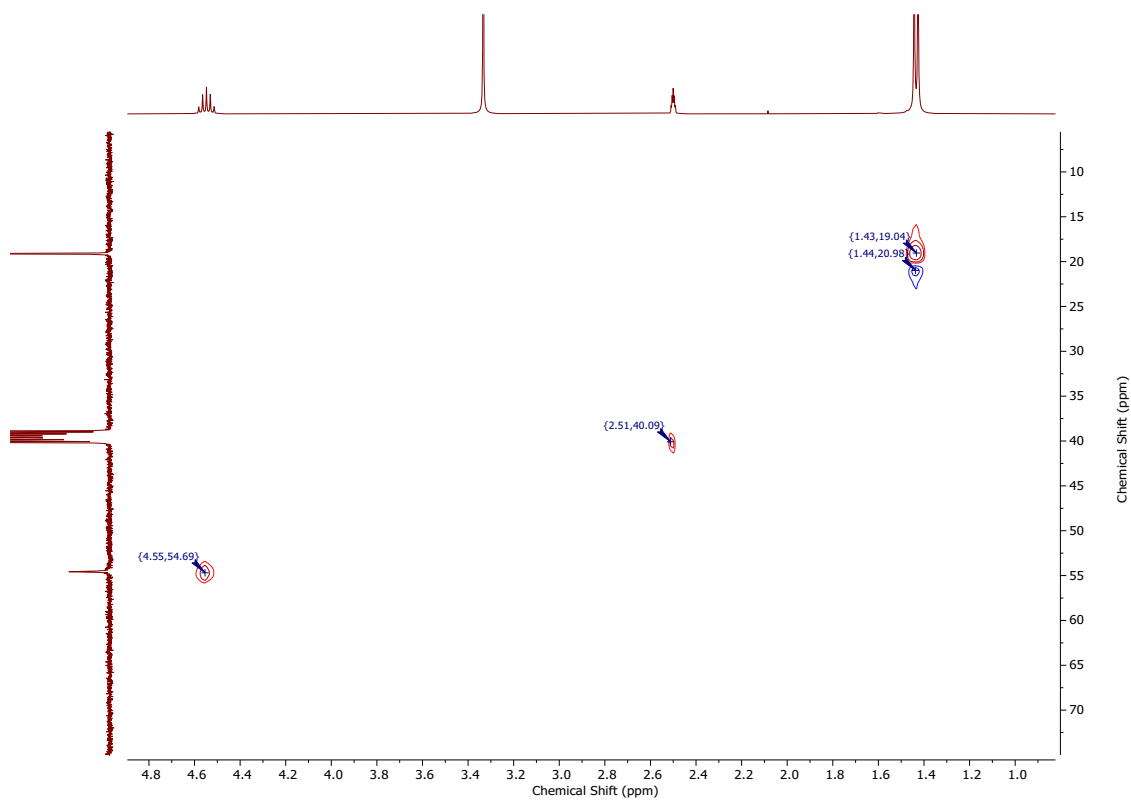


Figure S56: HSQC NMR spectrum of $[\text{AuCl}_2(\text{iPr}_2\text{dtc})]$ in DMSO-d_6 .

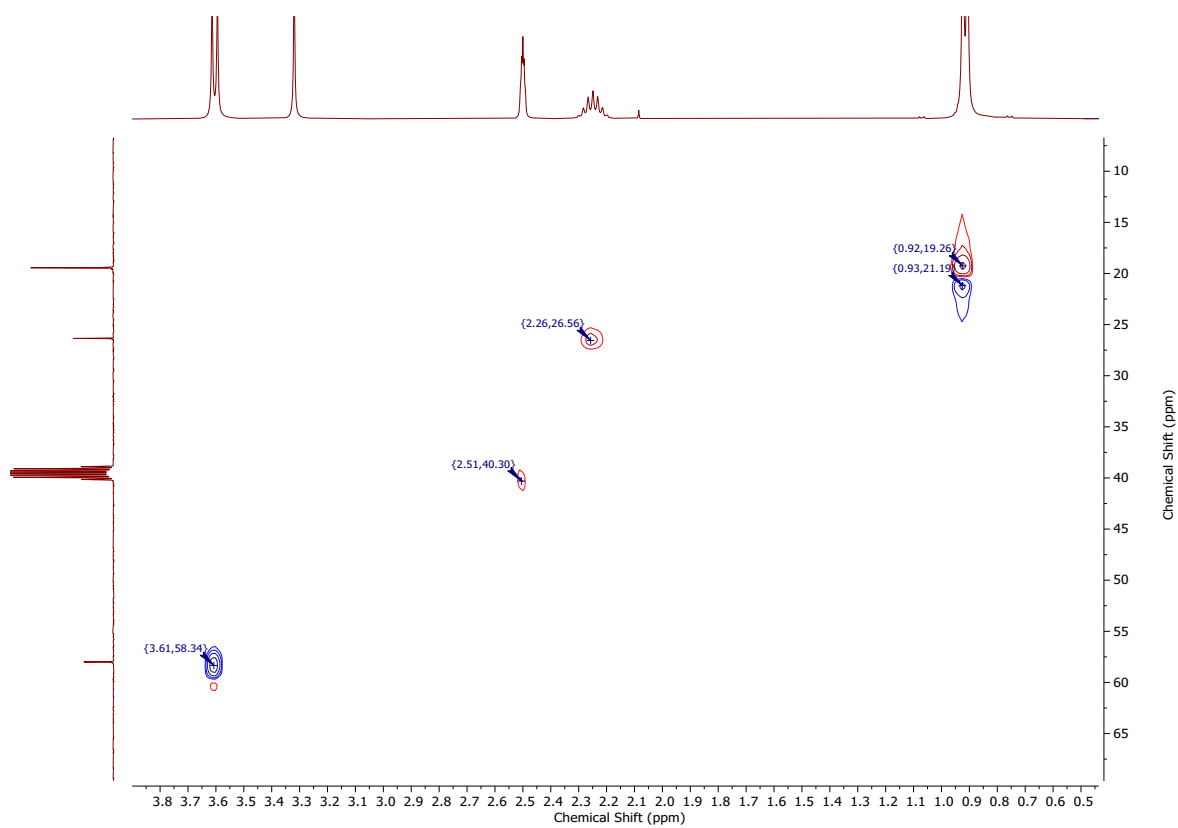


Figure S57: HSQC NMR spectrum of $[\text{AuCl}_2(\textit{i}\text{Bu}_2\text{dtc})]$ in DMSO-d_6 .

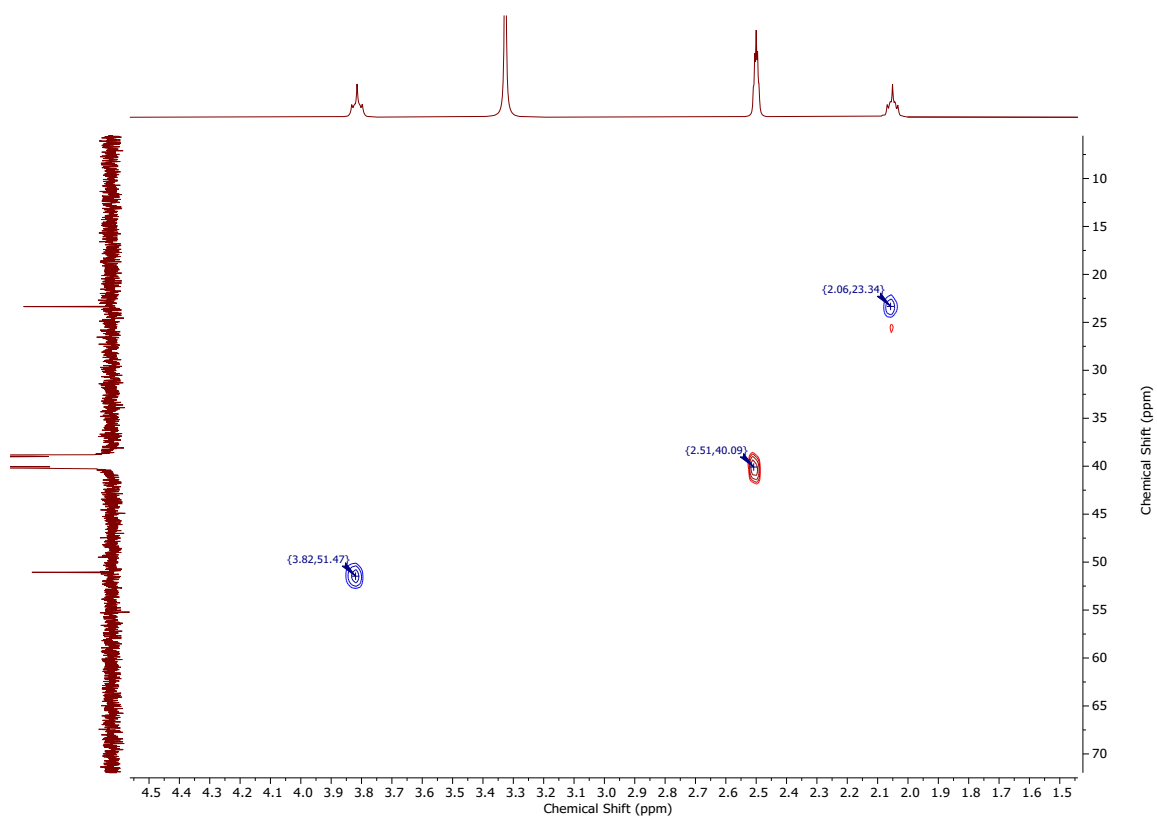


Figure S58: HSQC NMR spectrum of $[\text{AuCl}_2(\text{pyrr-dtc})]$ in DMSO-d_6 .

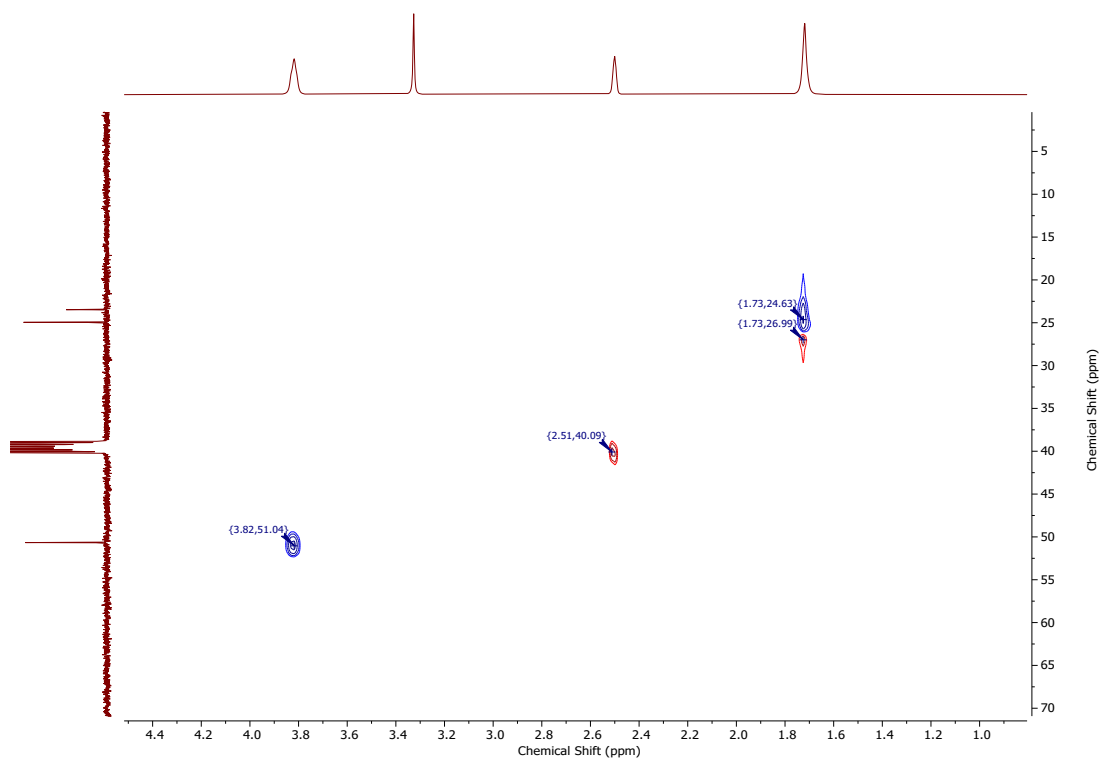


Figure S59: HSQC NMR spectrum of $[\text{AuCl}_2(\text{pip-dtc})]$ in DMSO-d_6 .

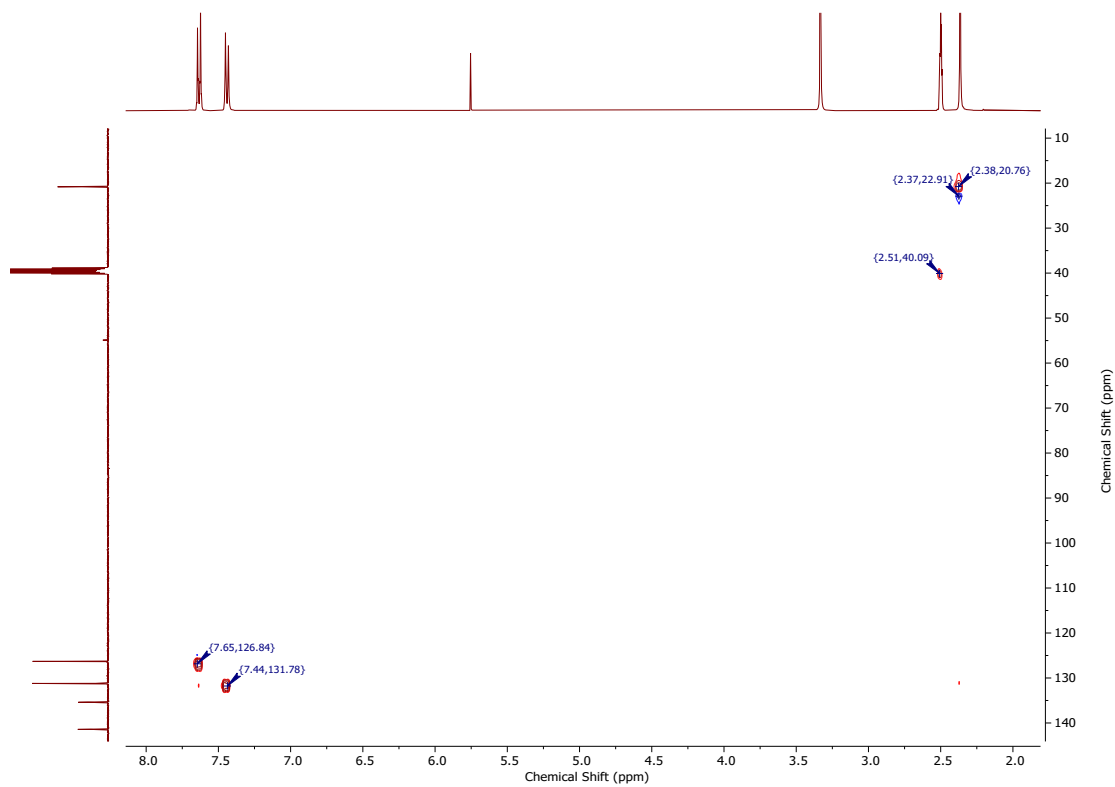


Figure S60: HSQC NMR spectrum of $[\text{AuCl}_2(\text{p-tolyl}_2\text{dtc})]$ in DMSO-d_6 .

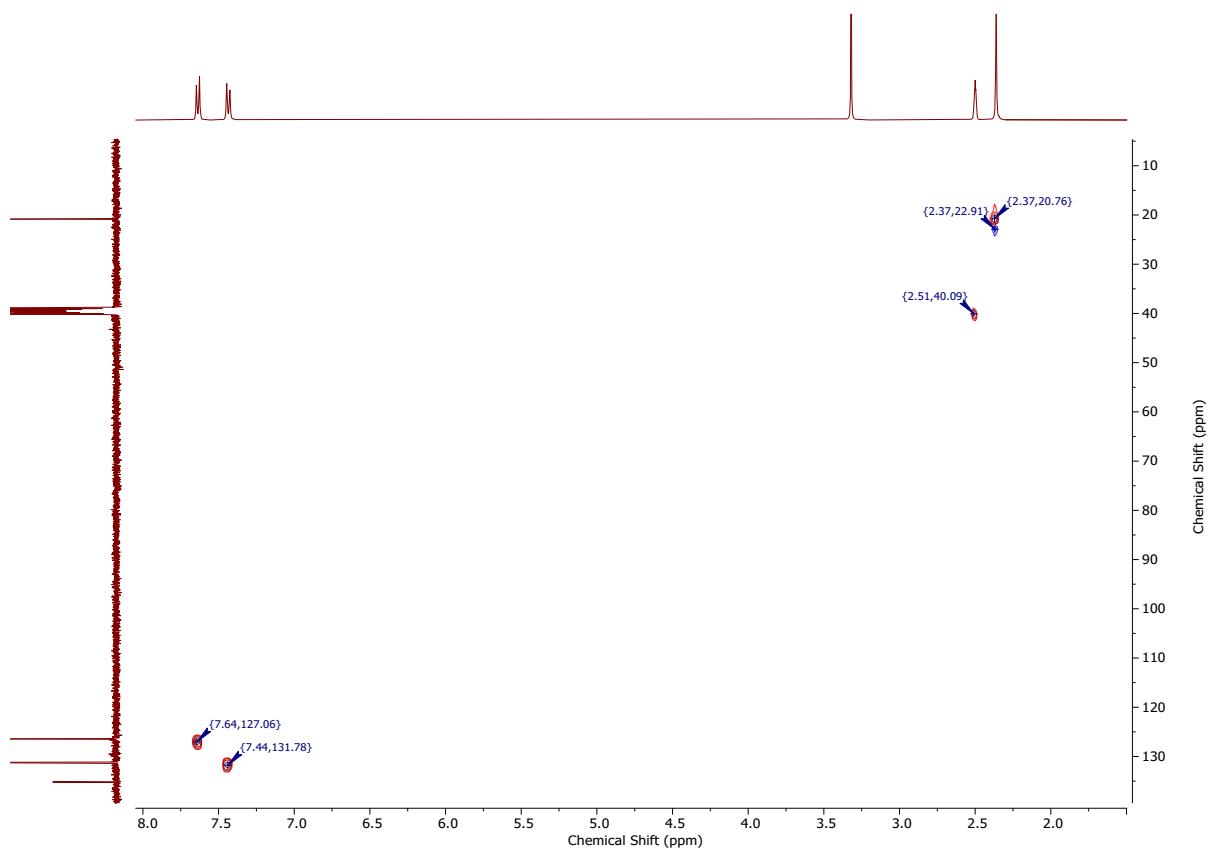


Figure S61: HSQC NMR spectrum of [AuBr₂(p-tolyl)₂dtc] in DMSO-d₆.

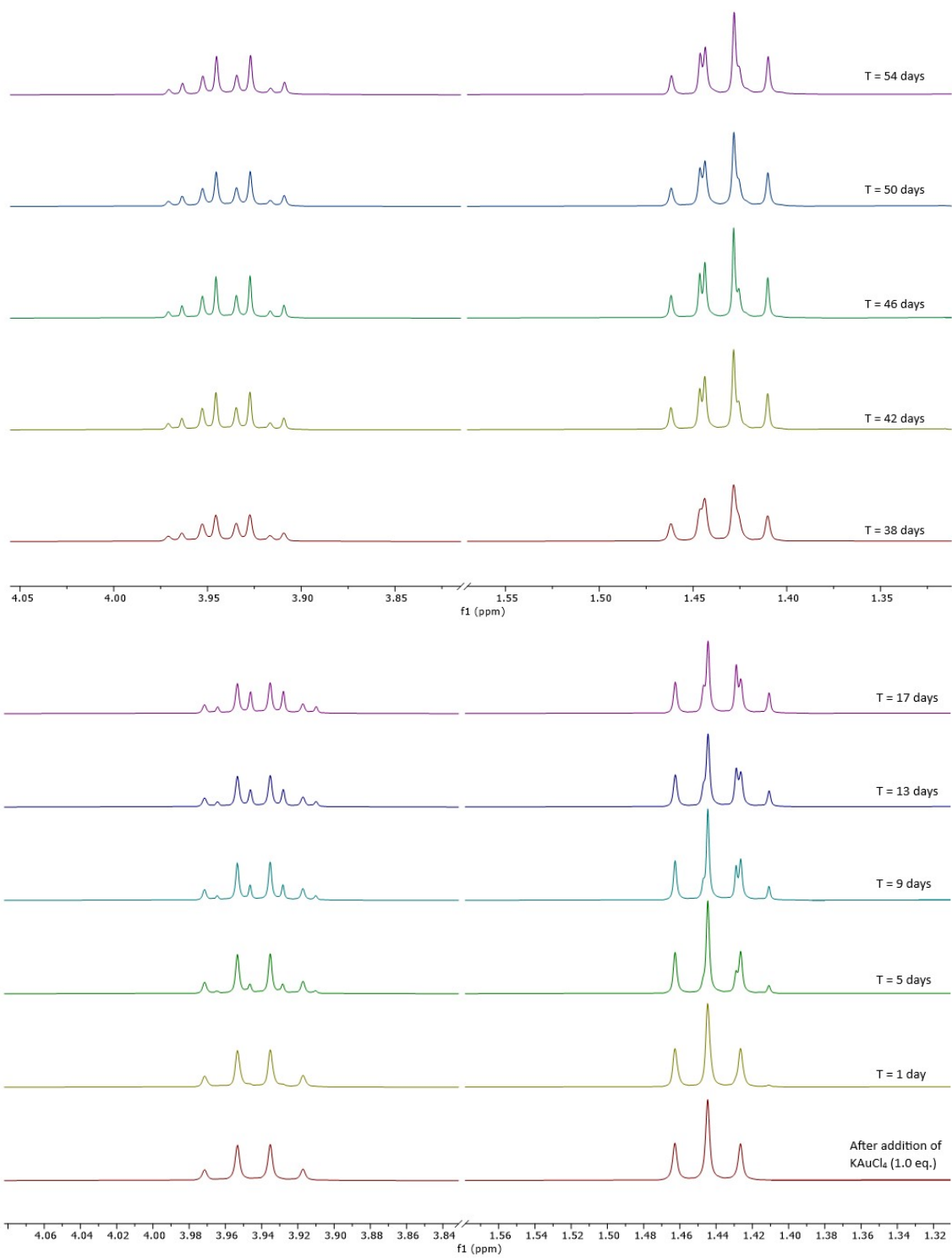


Figure S62: stacked plot of ^1H NMR spectra monitoring the “[$\text{AuCl}_2(\text{Et}_2\text{dtc})$]” mixture in acetone- d_6 , formed by adding one equivalent of KAuCl_4 to $[\text{Au}(\text{Et}_2\text{dtc})_2][\text{BF}_4]$.

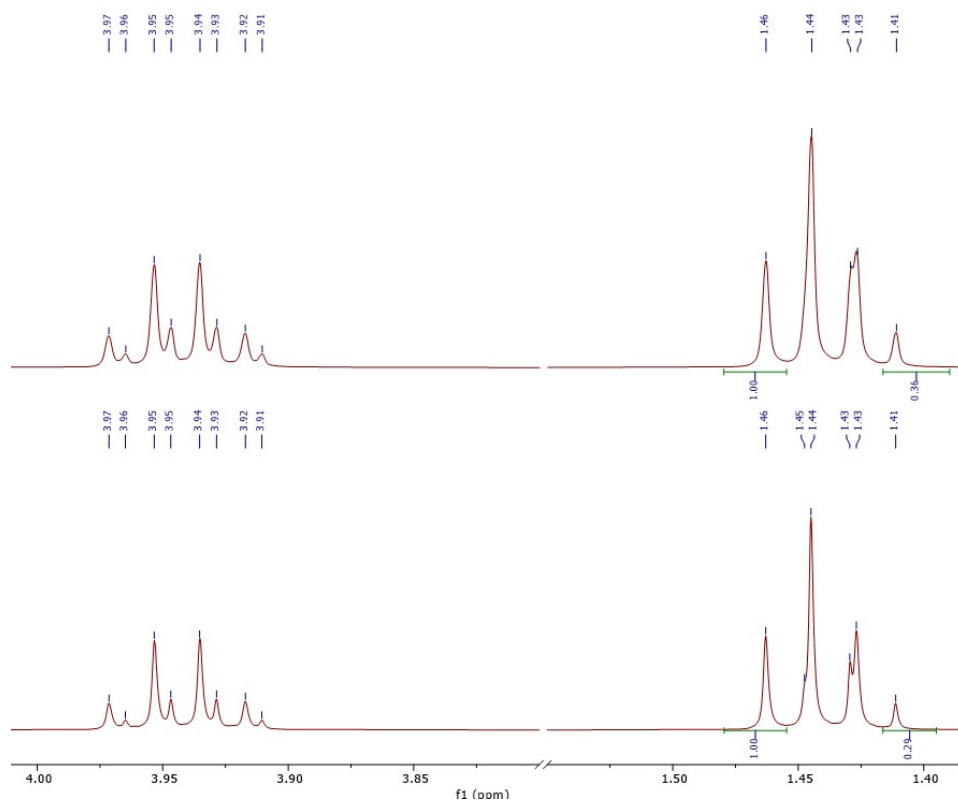


Figure S63: comparison of ^1H NMR spectra in acetone- d_6 showing the as-synthesized “[AuCl $_2$ (Et $_2$ dtc)]” mixture and after leaving it to stand for 24 hours.

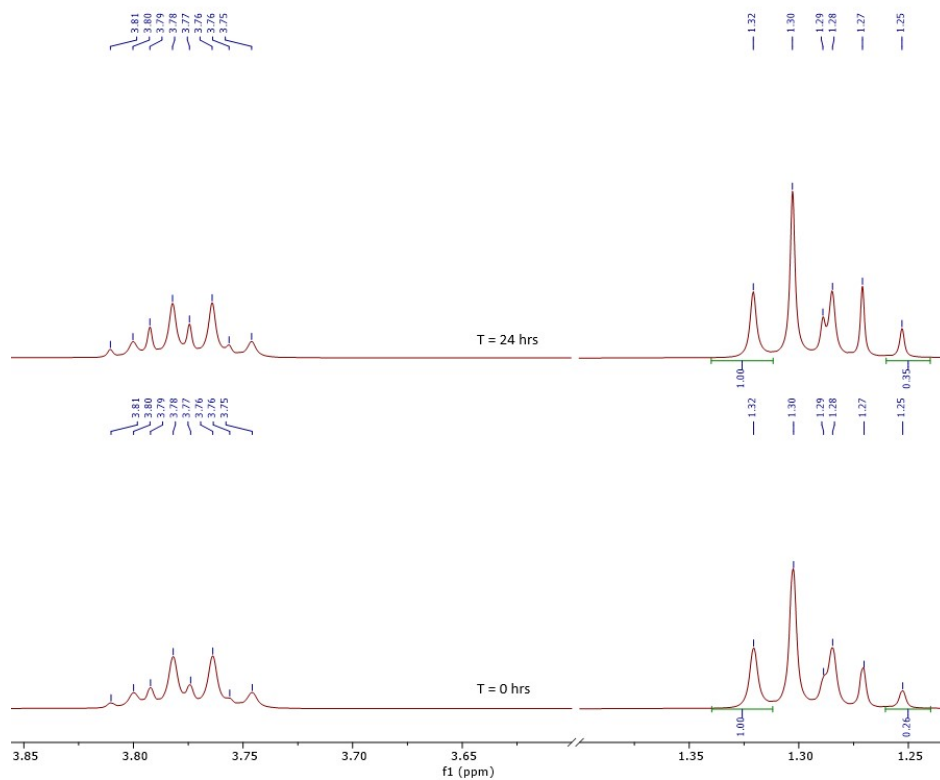


Figure S64: comparison of ^1H NMR spectra in DMSO- d_6 showing the as-synthesized “[AuCl $_2$ (Et $_2$ dtc)]” mixture and after leaving it to stand for 24 hours.

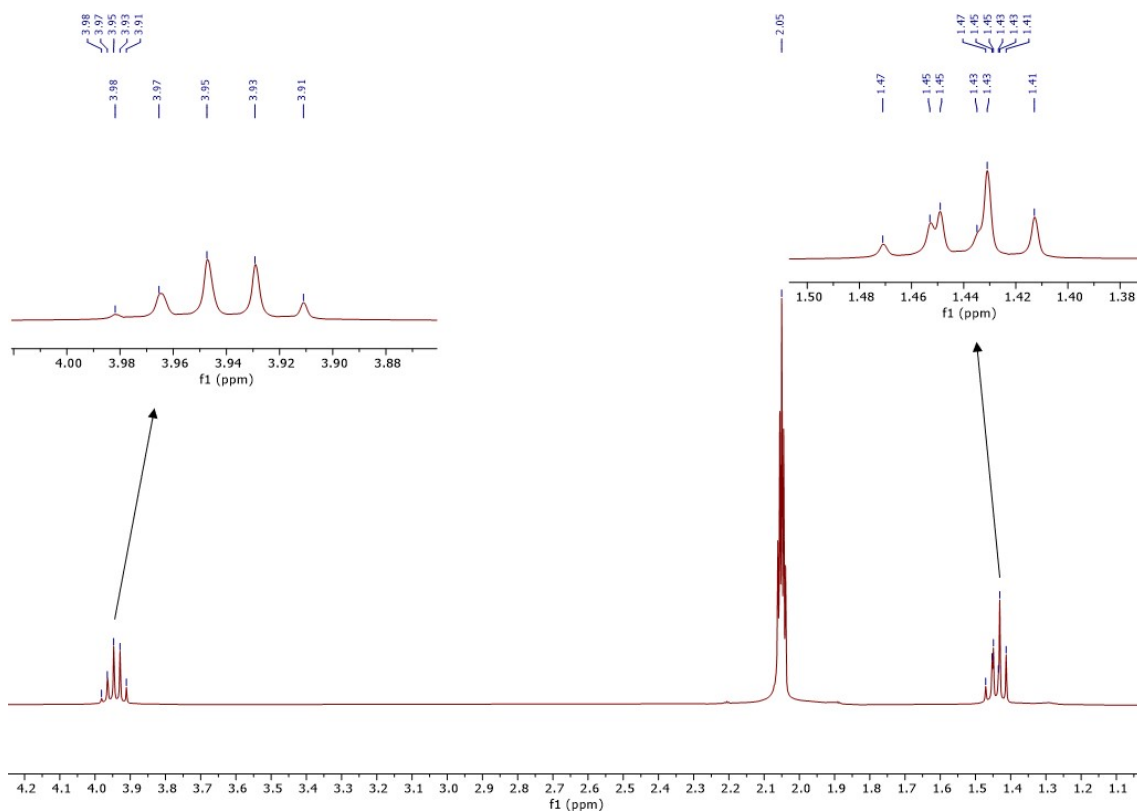


Figure S65: ^1H NMR spectrum in acetone- d_6 showing the as-synthesized “[AuCl₂(Et₂dtc)]” mixture from dilute acetone followed by a 72 hour reflux.

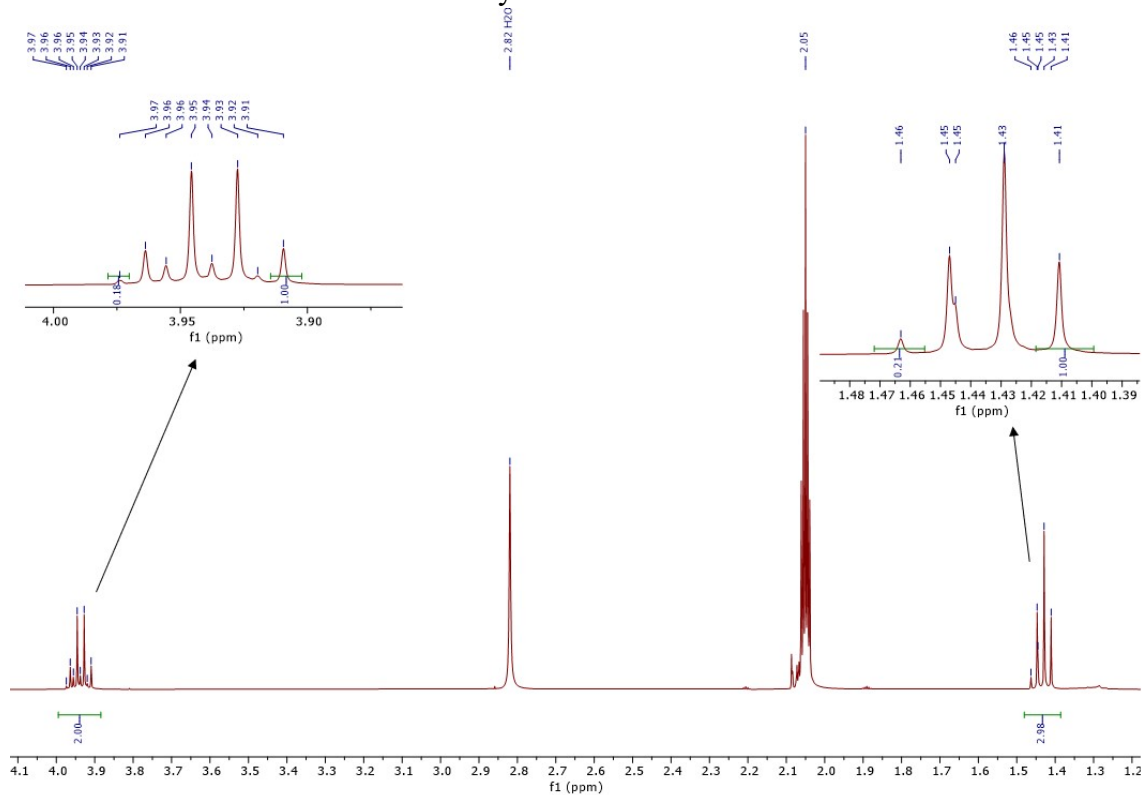


Figure S66: ^1H NMR spectrum in acetone- d_6 showing the as-synthesized “[AuCl₂(Et₂dtc)]” mixture from dilute refluxing acetone (our best synthetic conditions).

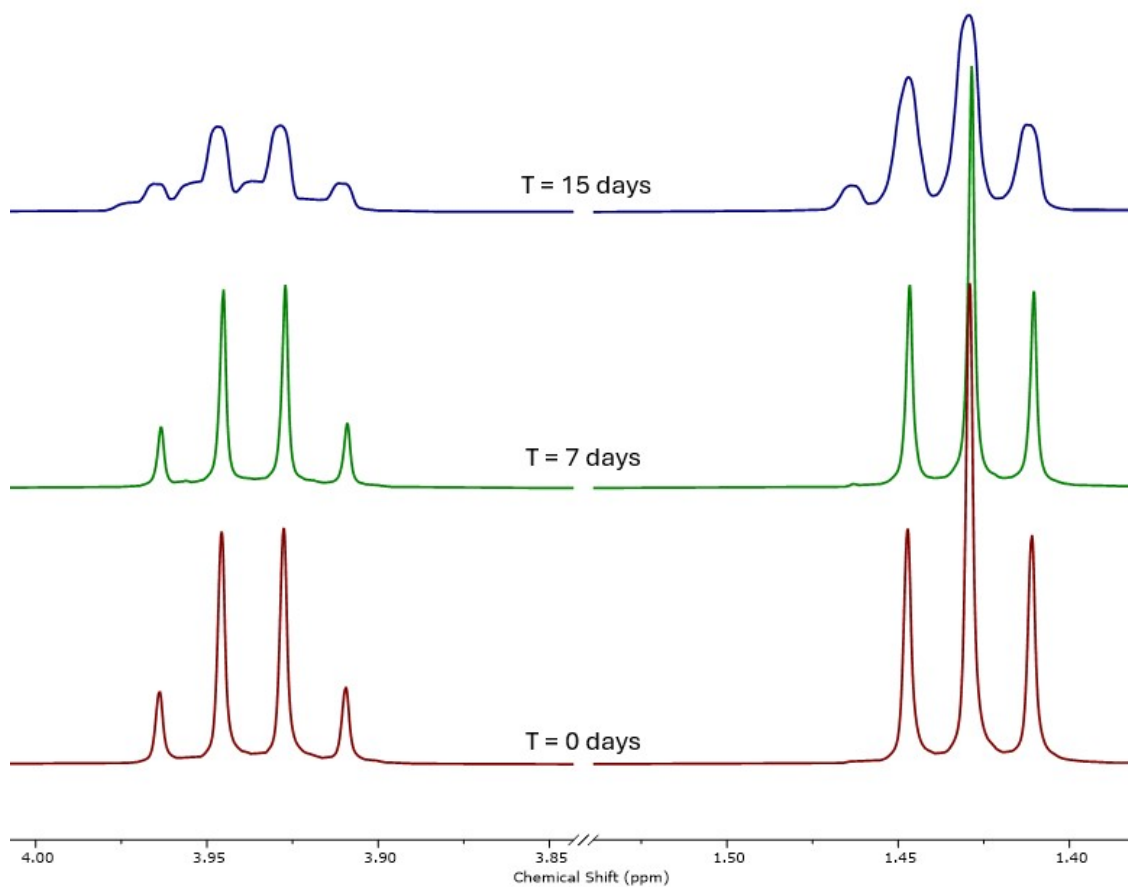


Figure S67: ^1H NMR spectrum in acetone- d_6 showing the “pure” $[\text{AuCl}_2(\text{Et}_2\text{dtc})]$ spectrum obtained from recrystallized material (red, $T = 0$ days) reverting to a mixture in solution (blue, $T = 15$ days).

4. Other Spectra

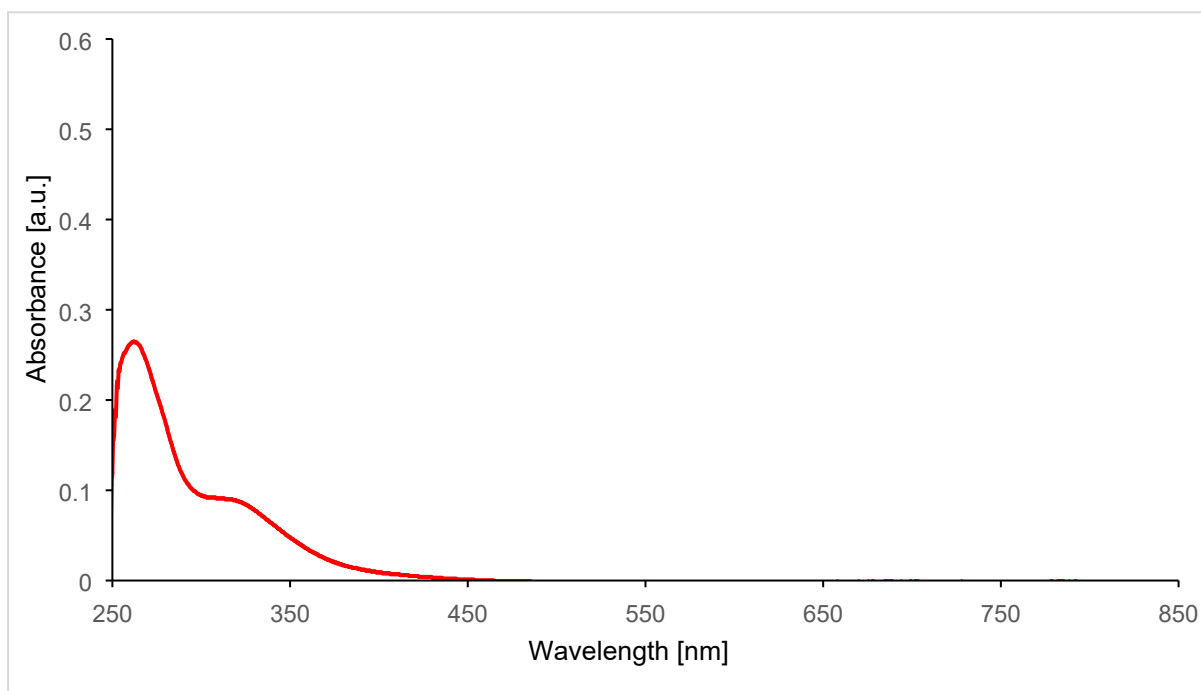


Figure S68: UV-vis spectrum of crystalline $[\text{AuCl}_2(\text{Et}_2\text{dtc})]$ dissolved in DMSO (1×10^{-5} M) with $\lambda_{\text{max}} = 262$ nm.

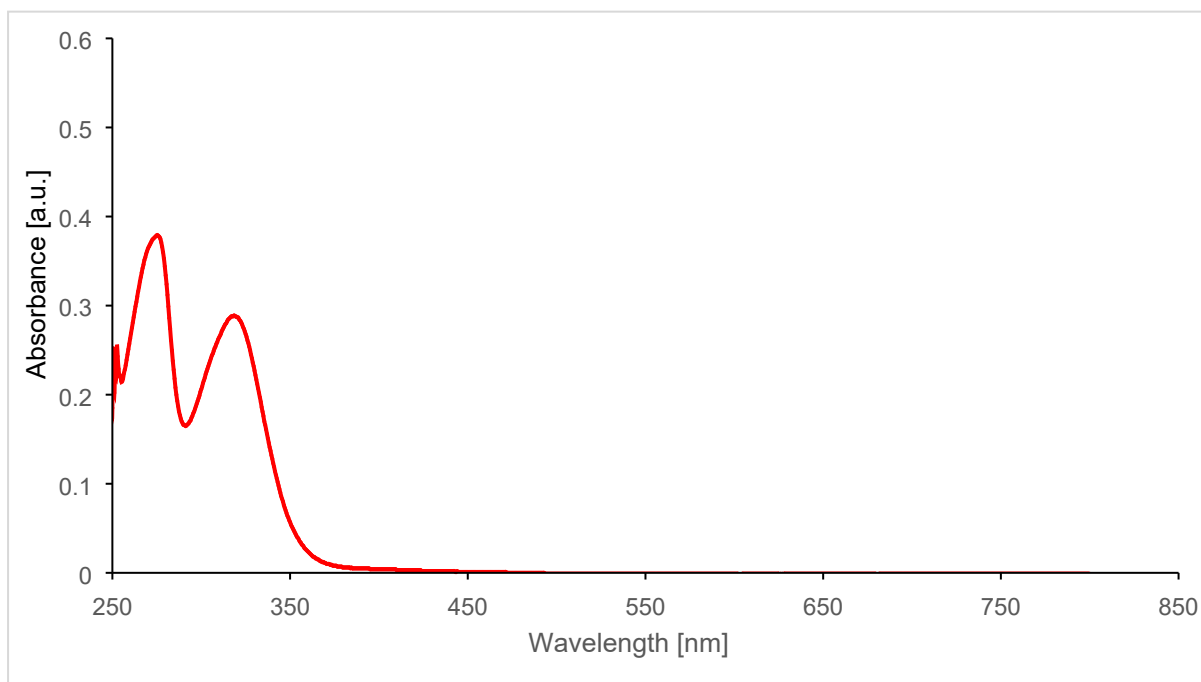


Figure S69: UV-vis spectrum of $[\text{Au}(\text{Et}_2\text{dtc})_2][\text{BF}_4]$ dissolved in DMSO (1×10^{-5} M) with $\lambda_{\text{max}} = 275$ nm.

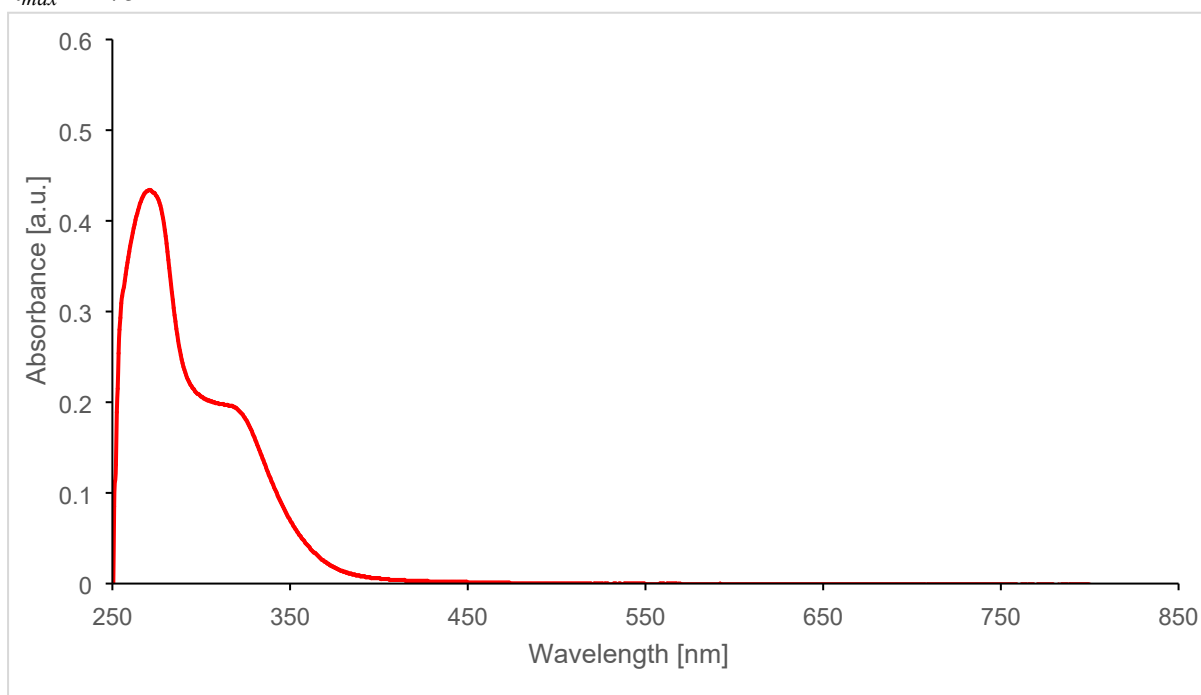


Figure S70: UV-vis spectrum of the as-synthesized “[$\text{AuCl}_2(\text{Et}_2\text{dtc})$]” ($\sim 3:5$ ratio of neutral:cationic) dissolved in DMSO (5 mg / L) with $\lambda_{\text{max}} = 271$ nm.

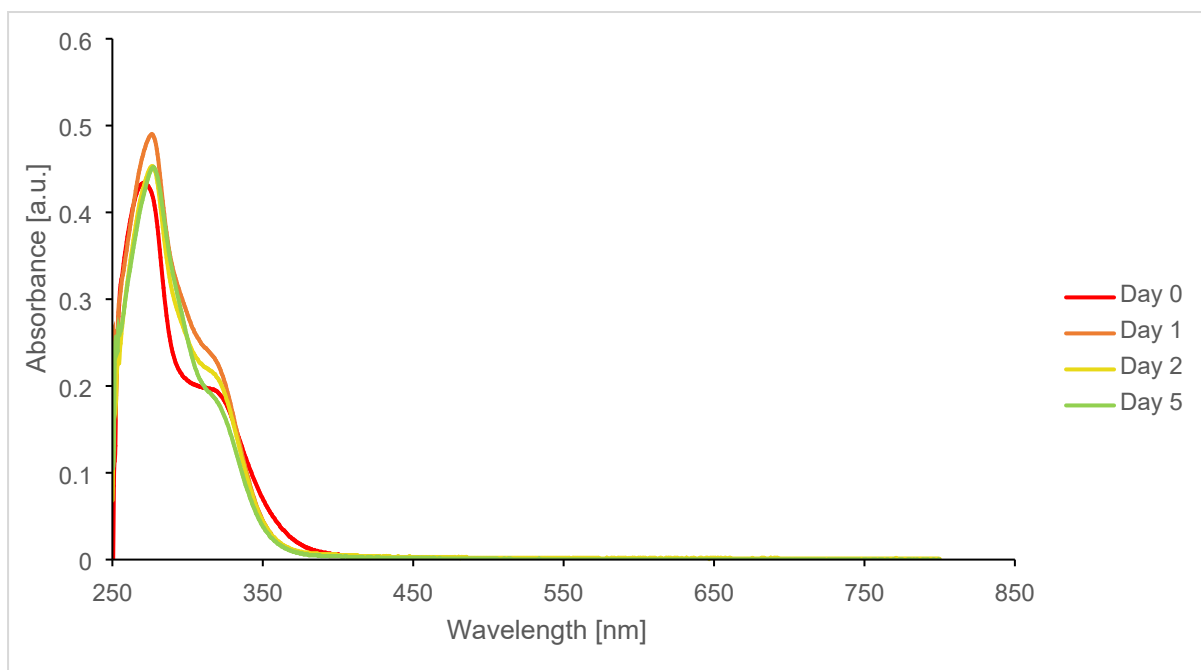


Figure S71: UV-vis spectra of the as-synthesized “[$\text{AuCl}_2(\text{Et}_2\text{dtc})$]” ($\sim 3:5$ ratio of neutral:cationic) dissolved in DMSO (5 mg / L) showing the decrease in secondary maximum at ~ 287 nm over time as the equilibrium shifts to favour the neutral species.

5. References

- S1) G. Hogarth. *Mini Rev. Med. Chem.*, 2012, **12**, 1202–1215.
- S2) A. Angeloski, J. M. Hook, M. Bhadbhade, A. T. Baker and A. M. McDonagh. *CrystEngComm*, 2016, **18**, 7070–7077.
- S3) F. Carta, M. Aggarwal, A. Maresca, A. Scozzafava, R. McKenna and C. T. Supuran. *Chem. Commun.*, 2012, **48**, 1868–1870.
- S4) R. Biswas, P. Thakur, G. Kaur, S. Som. M. Saha, V. Jhahria, H. Singh, I. Ahmed, B. Banerjee, D. Chopra, T. Sen and K. K. Haldar. *Inorg. Chem.*, 2021, **60**, 12355–12366.
- S5) R. T. Mertens, S. Parkin and S. G. Awuah. *Chem. Sci.*, 2020, **11**, 10465–10482.
- S6) J. C. Sarker, R. Nash, S. Boonrungsiman, D. Pugh and G. Hogarth. *Dalton Trans.*, 2022, **51**, 13061–13070.
- S7) R. Uson, A. Laguna, M. Laguna, D. A. Briggs, H. H. Murray and J. P. Fackler Jr. *Inorg. Synth.*, 1989, **26**, 86.
- S8) M. Morgen, P. Fabrowski, E. Amtmann, N. Gunkel and A. K. Miller. *Chem. Eur. J.*, 2021, **27**, 12156–12165.
- S9) S. J. Coles, D. R. Allan, C. M. Beavers, S. J. Teat and S. J. W. Holgate. Leading edge chemical crystallography service provision and its impact on crystallographic data science in the twenty-first century. In, *Structure and Bonding*, 2020, Berlin, Heidelberg. Springer 1–72.
- S10) CrysAlisPRO, Oxford Diffraction/Agilent Technologies UK Ltd, Yarnton, England.
- S11) O. V. Dolomanov, L. J. Bourhis, R. J. Gildea, J. A. K. Howard and H. Puschmann, *J. Appl. Cryst.* 2009, **42**, 339–341.
- S12) C. F. Macrae, I. Sovago, S. J. Cottrell, P. T. A. Galek, P. McCabe, E. Pidcock, M. Platings, G. P. Shields, J. S. Stevens, M. Towler and P. A. Wood. *J. Appl. Cryst.*, 2020, **53**, 226–235.
- S13) O. V. Loseva, T. A. Rodina, A. V. Ivanov, I. A. Lutsenko, E. V. Korneeva, A. V. Gerasimenko and A. I. Smolentsev. *Russ. J. Coord. Chem.*, 2018, **44**, 604–612.
- S14) I. Ymén. *Acta Cryst. Sect. C*, 1983, **C39**, 874–877.